5th AIAA Theoretical Fluid Mechanics Conference
23 - 26 June 2008, Seattle, Washington

AIAA 2008-4348

Level of Turbulence Intensity Associated with Bluff-Body Separation for Large Values of the Reynolds Number

Bernhard Scheichl* and Alfred Kluwick†

Vienna University of Technology, A-1040 Vienna, Austria

The paper concerns a rational and physically feasible description of gross separation from the surface of a plane and more-or-less bluff obstacle in an incompressible and otherwise perfectly uniform stream for arbitrarily large values of the globally formed Reynolds number. The analysis is initialized by a remarkable conclusion drawn from recent theoretical results that is corroborated by experimental findings but apparently contrasts common reasoning: the attached boundary layer extending from the front stagnation point to the position of separation at the body surface never attains a fully developed turbulent state, even in the limit of infinite Reynolds number. As a consequence, the boundary layer exhibits a certain level of turbulence intensity that is determined by the separation process governed by locally strong viscous/inviscid flow interaction. This mechanism is expected to be associated with rapid transition of the separating shear layer towards an almost fully developed turbulent state. Here a rigorous asymptotic analysis, essentially carried out without resorting to a specific turbulent closure and supported by a numerical investigation, of the topology of the boundary layer flow close to separation is presented.

Nomenclature

ℓ	Mixing length shape function, see Eq. (85)
$\mathcal{C}$	Curve of free streamline of potential flow
$\mathcal{F}$	Front stagnation point
$\mathcal{G}$	Point of the Goldstein singularity
$\mathcal{R}$	Rear stagnation point
$\mathcal{S}$	Separation point of potential flow
$\mathbf{q}$	Pseudo-vector, used to abbreviate the expansions (21), (31), (40)
$\mathbf{u}$	Velocity vector, see figure 1 (a)
A	Displacement function, see Eqs. (72), (80)
a	Coefficients in expansions (49), (66)
B	Intercept of $\mathcal{O}(1)$ in logarithmic law of the wall, see Eqs. (28), (34), (87)
b	"Bias" $\partial u_e/\partial x$ as $x \to 0_+$
C	Chord length
c	Coefficient (drag/lift)
D	Intercept of $\mathcal{O}(1)$ in logarithmic law of the wall for stagnating flow, see Eq. (37)
E	Quantity of $\mathcal{O}(1)$, entering skin-friction law (38)
F	Defect function, see Eq. (29)
f	Local similarity solution, see Eqs. (63)–(66)
G	Defect function for stagnating flow as $x \to 0_+$, see Eq. (33)
H	Hiemenz flow function, see Eq. (14)

*Postdoctoral Research Fellow, Vienna University of Technology, Institute of Fluid Mechanics and Heat Transfer, Resselgasse 3/E322, A-1040 Vienna, Austria, e-mail: b.scheichl@tuwien.ac.at.

†Full Professor, Vienna University of Technology, Institute of Fluid Mechanics and Heat Transfer, Resselgasse 3/E322, A-1040 Vienna, Austria, e-mail: a.kluwick@tuwien.ac.at, Senior member of AIAA.

h Surface metric coefficient
i Counter
J Reynolds shear stress function as $x \to 0_+$, see Eq. (33)
K Coefficient in expansions of F_1^* and B_1, see Eqs. (52), (53)
k BV parameter
l Mixing length shape function, see Eqs. (85)–(87)
M Kummer's confluent hypergeometric function
p Time-mean pressure
R Global reference length, given by radius of cylinder
r Radius, see Eq. (8)
Re Reynolds number, see Eq. (1)
S Reynolds shear stress function, see Eq. (29)
s Local streamwise coordinate, see Eq. (7)
T Turbulence-level gauge parameter
U Global reference velocity, i.e. velocity of oncoming parallel flow
u Time-mean velocity component in x-direction
v Time-mean velocity component in y-direction
W Wingspan length
X Stagnation-flow coordinate in x-direction
x Distance along body surface measured from $\mathcal{F}$
Y BL coordinate, see Eq. (11)
y Distance perpendicular to body surface

Subscripts

$\mathcal{C}$ Value along $\mathcal{C}$
$\mathcal{F}$ Value at $\mathcal{F}$
$\mathcal{G}$ Value at $\mathcal{G}$
$\mathcal{R}$ Value at $\mathcal{R}$
$\mathcal{S}$ Value at $\mathcal{S}$
b Base of outer defect layer
C Chord Reynolds number, here $\tilde{C}$ replaces $\tilde{R}$ in Eq. (1)
D Drag
e Velocity of external flow evaluated at surface, acting on the BL edge
i i-th term of asymptotic expansion, i standing for $0, 1, 2, \ldots$
ij j-th term in i-th term of asymptotic expansion, i and j standing for $0, 1, 2, \ldots$
L Lift
max Maximum value
min Minimum value
p Particular solution
q Derivative with respect to q, here standing for x, y, Y, η
t Total shear stress, see Eq. (19)

Conventions

BL Boundary layer
BV Brillouin–Villat
ODL Outer defect layer, see figure 3
VWL Viscous wall layer, see figure 3
q^* q meaning any quantity of $\mathcal{O}(1)$, representative for sublayer of outer defect region, see § III.B.1
$\bar{q}$ q meaning any quantity of $\mathcal{O}(1)$ satisfying linearized BL problem as $s \to 0_-$, see Eqs. (57), (59)–(61)
$\hat{q}$ q meaning any quantity of $\mathcal{O}(1)$, representative for nonlinear flow region, see § III.B.3
I_i Modified Bessel function of order i, $i = 0, 1$, see Eq. (54)
K_i Modified Bessel function of order i, $i = 0, 1$, see Eq. (54)
u', v' Turbulent fluctuations of u, v
u_T Turbulent reference velocity, see Eq. (17)
$\langle \cdots \rangle$ Reynolds-averaged quantity, latter indicated by dots

Symbols

α Gauge function, see Eq. (62)
β Constant in closure for $l+$, see Eq. (87)
χ Perturbation parameter, see Eq. (29)
Δ Scaled thickness of turbulent BL, see Eq. (30)
δ Relative thickness of turbulent BL, see Eq. (30), figure 1 (b)
ϵ Gauge function, see Eq. (22)
ε Constants of $\mathcal{O}(1)$ in near-wall behavior of Σ^+ and Ψ^+, see Eq. (25), (26)
η Turbulent BL coordinate, see Eq. (30)
Γ Quantity in closure for $l+$, see Eq. (87)
γ Gauge function measuring velocity defect, see Eq. (22), figure 1 (b)
ι Similarity variable of Goldstein region, see Eq. (84), figure 3
κ V. Kármán constant, see Eq. (28)
$\varkappa$ Surface curvature
Λ Coefficient determining wall shear perturbation, see Eq. (65)
λ Gauge function, see Eq. (40)
ν Kinematic viscosity
Ω Reduced wall shear, see Eq. (88), figure 5
ω Constant governing Goldstein singularity, see Eqs. (81)–(83), (89)
Φ Total head in Bernoulli's equation (79)
ϕ Arc angle, measuring position on cylinder surface from $\mathcal{F}$
φ Constant in closure for $l+$, see Eq. (87)
π Gauge function, measuring pressure gradient, see Eq. (58)
Ψ Stream function for BL, see Eq. (11)
ψ Stream function
Σ Reynolds shear stress function, see Eq. (11)
σ Perturbation parameter, see Eq. (29)
τ Perturbation parameter, see Eq. (38)
θ Local polar angle, see Eq. (8)
ϑ Variable of integration
Υ Displacement thickness, see Eq. (88), figure 5
ϱ Density
Ξ "Bias" $\mathrm{d}\Delta_1/\mathrm{d}x$ of thickness of turbulent BL as $x \to 0_+$, see Eq. (33)
ξ Goldstein coordinate in x-direction, see Eq. (81)
ζ Local similarity variable, see Eq. (63)

Superscripts

$'$ Derivative
$+$ Quantity expressed in wall layer scaling, see Eq. (16)
$\sim$ Dimensionful quantity
$\breve{\eta}$ Reduced η, see Eq. (54)

I. Introduction

NOTWITHSTANDING its principal importance for providing a sound basis to predict the extremes of safe flight conditions (i.e. of drag and lift), as well as effective methods of flow control, the rational time-mean description of massive BL separation from a relatively thick airfoil must, unfortunately, still be regarded as one of the most challenging unsolved basic problems in theoretical fluid mechanic. We shall be concerned with this issue in the present paper, where, for the sake of simplicity and clearness, the analysis is restricted to incompressible nominally steady and two-dimensional flow of a fluid with uniform density and viscosity.

I.A. Motivation

The answer to the question, what really has hampered so far a rigorous treatment of this fundamental problem, is probably provided by the fact that it essentially comprises five particular issues, each of them undoubtedly posing a challenge, and their rather complex interplay:

(i) the asymptotically correct picture of the flow past a curved obstacle (having a smooth impermeable

rigid surface) on a spatial scale comparable with the body dimensions as the governing parameter, namely the globally formed Reynolds number, Re, takes on arbitrarily large values;

(ii) the presumably locally concentrated mechanism of transition of the originally laminar flow near the leading-edge or front stagnation point $\mathcal{F}$ towards a more-or-less pronounced turbulent BL further downstream as $Re \to \infty$;

(iii) the asymptotic structure of the attached portion of the BL downstream of the location of transition;

(iv) the development of a local asymptotic theory of self-induced separation, which (presumably) in essence requires the description of strong BL interaction, allowing for a gradual transformation of the BL into a separated shear layer;

(v) finally, the description of the separated-flow regions (i.e. separated shear layer, weakly recirculating separated flow region in the lee side of the obstacle, downstream-evolving wake flow).

An attempt to rigorously tackle the questions (i)–(iii) has been made by the authors in a recent preceding study, see Ref. 1. First, there they have (convincingly) outlined that in the limit $Re \to \infty$ the time-averaged global flow is to be sought in the class of the well-known Helmholtz-Kirchhoff-type flows that exhibit free streamlines which depart smoothly from the surface in $\mathcal{S}$.[2,3] Secondly, the authors have seized a physically appealing suggestion to cope with the ab initio unknown level of turbulence intensity – or, equivalently, the order of magnitude of the Reynolds stresses – in the part of the BL that stretches from $\mathcal{F}$ to the position of separation, which must be attributed to Neish and Smith, see Ref. 4: in that previous work on the BL flow past a bluff body flow a classical, i.e. Prandtl-type, BL-formulation is adopted, where the included Reynolds shear stress is assumed to be proportional to a so-called turbulence intensity gauge factor, T, that may assume arbitrarily large values also as $Re \to \infty$.

Amongst others, it has been demonstrated in those preceding studies that in the limit $T \to \infty$ the BL structure is closely related to that of a fully developed turbulent BL which is characterized by the commonly accepted two-tiered asymptotic splitting.[5] As has been pointed out in Refs. 4, 6, this type of a turbulent BL refers to firmly attached flows only, as the interplay between the small relative streamwise velocity deficit of $\mathcal{O}(1/\ln Re)$ in the outer main layer and the comparatively transcendentally thin viscous wall layer is found to preclude a rational description of separation on the basis of first principles (a brief rationale is presented in § V). On the other hand, by considering the aforementioned "mixed" laminar-turbulent BL[1,4] in the limit $T \to \infty$, the velocity deficit is seen to be of $\mathcal{O}(1/\ln T)$, whereas the ratio of the thicknesses of the outer and the wall layer is of $\mathcal{O}[(\ln T/T)^2]$. Most important, as already indicated in Ref. 4, it is very likely that the in item (iv) above raised demand to devise a local interaction theory then can be accomplished on condition that T essentially shows a specific algebraic dependence on Re as $Re \to \infty$. Furthermore, in striking contrast to the well-established local asymptotic theory of purely laminar separation,[7,8] in the turbulent case the well-known so-called BV condition (namely, of an asymptotically weak BV singularity of the potential flow in $\mathcal{S}$) does not hold, despite some close formal resemblances the formulation of the underlying triple-deck problem is expected to bear.

Instead of directly focussing on this particular distinguished limit and the associated local description of separation (and, in turn, heading to the above point (v) then), we feel it much more instructive to initially elucidate the further differences and analogies between the behavior of purely laminar BL flow and that assumed in the large-T limit as separation is approached. Thus, this paper deals with the BL equations in the limit $T \to \infty$, where the driving external Kirchhoff-type flow is parametrized by the so-called BV parameter k that measures the strength the BV singularity and its position on the obstacle surface, indicated by $\mathcal{S}$. The solutions of the BL equations are found to terminate in form of a Goldstein-type singularity[9,10] taking place at $\mathcal{G}$, upstream of $\mathcal{S}$, for $T \geq 0$. Hence, particular emphasis is placed on highlighting the local structure of this singular behavior in dependence of k as $T \to \infty$, when $\mathcal{G}$ approaches $\mathcal{S}$. Since the flow description presented here solely relies on the BL approximation, it is, therefore, inevitably accompanied by the occurrence of those singularities. That is, it is rendered uniformly valid (and physically realistic) except within an asymptotically small region encompassing both singularities in the limit $T \to \infty$. We note that an asymptotically correct global formulation of the separation process then will be completed in a subsequent separate treatment of the above quoted topics (iv) and (v).

I.B. Status Quo of Research

Before we commence the analysis as suggested above, it is useful to first itemize the most important preliminary results it is based on.

- It is well-known that the potential flow past a more-or-less blunt body (with a, respectively, smooth, wedge-, or cusp-shaped trailing edge) that exhibits free streamlines (confining an open or closed cavity) can be mapped onto that about a circular cylinder by means of conformal mapping. Also, the structure of the attached BL flow that stretches from $\mathcal{F}$ to $\mathcal{G}$ is found to be qualitatively independent of the specific distribution of the imposed pressure gradient for all positive values of T.[1] Most important, in the limit $T \to \infty$ the local behavior of the solutions of the BL equations immediately upstream of $\mathcal{G}$ depends essentially only on the structure of the BV singularity.[2,3] As a consequence, any local and global theories that cope with the issues (iv) and (v) above are expected to predict all the properties which are important for a comprehensive understanding of break-away separation independently of the specific choice of the imposed Kirchhoff-type flow. Therefore, the case of a circular cylinder, exposed to strictly uniform cross flow, is supposed to provide the "canonical" situation, sketched in figure 1 (a). In turn, the Reynolds number is introduced in the form

$$Re := \tilde{U}\tilde{R}/\tilde{\nu} \to \infty. \tag{1}$$

  Note that is assumed in figure 1 (a) that the Goldstein singularity takes place upstream of $\mathcal{S}$ and (coincides asymptotically with the separation point.

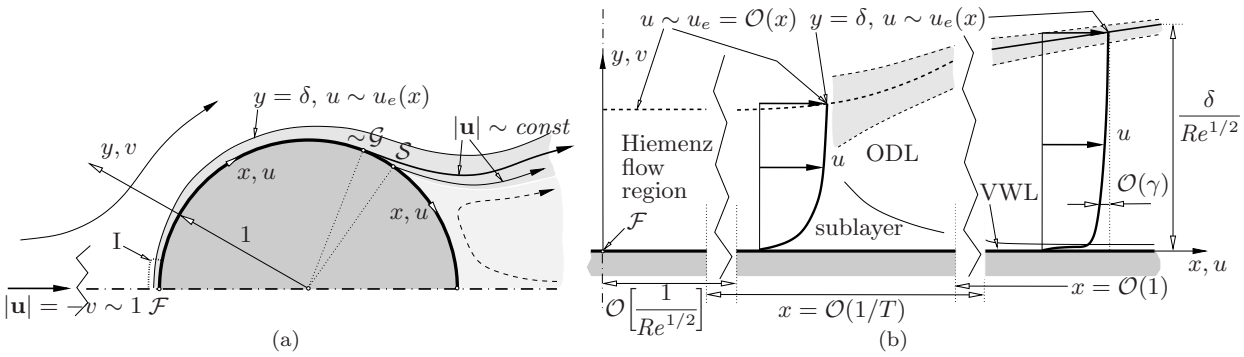

Figure 1. Flow configuration (non-dimensional representation, curvilinear coordinates x, y): (a) global (canonical case, dark-shaded region: BL and separated shear layer, light-shaded region, broken streamline: weakly recirculating flow), (b) region I, asymptotic splitting in the limit $T \to \infty$ near $\mathcal{F}$ (shaded: viscous superlayer, not considered here).

- In the following, we consider an attached BL that behaves "as turbulent as possible", such that T is "as large as possible" as $Re \to \infty$. However, it is interesting to note that the numerical analysis of the BL equations put forward in Ref. 1 points to a second, different picture of massive separation in the limit (1), not pursued further here (cf. § IV.B): in that case, both k and T assume specific (positive) values, such that the Goldstein singularity is vanishingly weak and, simultaneously, $\mathcal{G}$ coincides with $\mathcal{S}$. We note that, for the time being, it is fully unclear whether this limiting solution of the BL equations allows for a self-consistent flow description.

- The analysis of the contrasting case $T \to \infty$ presented in Ref. 1 strongly suggests a rather remarkable property of BL flow issuing from a stagnation point, namely, that T is bounded from above by $\mathcal{O}(Re^{1/2})$. Most important, the (hypothetical) limit $T = Re^{1/2}$ refers to a fully developed turbulent BL that exhibits the well-known two-layer structure,[5] which is essentially governed by perfect equilibrium between the wall shear stress and the sum of the molecular and the turbulent stresses. In that case, however, the Reynolds-averaged Navier–Stokes equations, non-dimensional with $\tilde{U}$, $\tilde{R}$, $\tilde{\nu}$, and the density $\tilde{\varrho}$, would be fully retained (except for curvature effects) in the limit (1) in a square region showing an extent of $\mathcal{O}(Re^{-1/2})$ close to $\mathcal{F}$. The thereby reduced Reynolds number, relevant for the flow in this small region, then has the value 1. Therefore, it is rather unlikely that transition towards fully developed turbulence can develop there. Consequently, we expect a BL type flow in a

region which stretches of $\mathcal{O}(1/T)$ from $\mathcal{F}$, i.e. of asymptotically larger extent than that normal to the wall of $\mathcal{O}(Re^{-1/2})$. We will revert to this consideration in connection with the analysis given in § II.

- Hence, it has been demonstrated in Ref. 1 that this flow, associated with a slightly "underdeveloped" turbulence intensity level ($T \ll Re^{1/2}$), gives rise to a BL that still exhibits the conventional two-tiered asymptotic splitting, known from a fully developed turbulent BL ($T = Rey^{1/2}$),[5] as it evolves along the obstacle surface. The resulting flow splitting is shown in figure 1 (b), where the scalings are derived in § III.A. It is found, amongst others, that the (non-dimensional) BL thickness is of $Re^{-1/2}T/\ln T$. However, the order of magnitude of T in terms of Re as $T \to \infty$ is not known in advance but is expected to be fixed by the answer to the issue (iv) given in § I.A. Here, two strategies are possible to follow, in principle: first, the case $k > 0$ but independent of T, considered in the following. The second possibility assumes $k \to \infty$ as $T \to \infty$ and is tied in with the analysis of trailing-edge flow presented in Refs. 4,6. That is, in the latter case the imposed potential flow is considered as the slightly perturbed well-known strictly attached inviscid-flow solution, having a rear stagnation point $\mathcal{R}$. This will be pursued further in a different study.

- Indeed, the wind tunnel experiments carried out by Schewe[11] strongly suggest that the BL indeed never attains a fully developed turbulent state, even for arbitrarily large values of Re_C. This remarkable (although still tentative) conclusion is drawn from the visualization of oil flow film measurements of the separating flow past the suction side of a more-or-less plane and thick airfoil (aspect ratio $\tilde{W}:\tilde{C} = 6:1$, angle of attack of 12°). Let us first consider the distributions of the drag and lift coefficients c_D and c_L, respectively, shown in figure 2 on the following page (b): here the typical jump-like changes for $Re_C \approx 3.5 \times 10^5$ (associated with hysteresis effects, as indicated by arrows), $Re_C \approx 2.5 \times 10^6$, and $Re_C \approx 7.5 \times 10^6$ reflect the transitions from so-called sub- to trans-, trans- to super-, and, finally, super- to postcritical BL flow, cf. Ref. 12; the extents of these particular flow regimes are indicated by vertical dotted lines. The first three of these notations are commonly adopted to categorize bluff-body flow by attempting to isolate the location of transition to a developed turbulent shear layer, namely – in order of their appearance – downstream, in the immediate vicinity of, and upstream of the position of time-mean separation. In the supercritical regime the location of transition is apparently shifted towards $\mathcal{F}$ as Re_C increases. The postcritical flow is usually believed to be topologically equivalent to its asymptotic state, assumed in the limit $Re_C \to \infty$, as transition then already takes place close to $\mathcal{F}$.[12] Consequently, one is tempted to argue that the upper and lower snapshots of the instantaneous flows displayed in figure 2 (a) refer to, respectively, trans- and fully turbulent supercritical, i.e. postcritical, BL flows. In the first case transition of the separating laminar BL towards a separated turbulent shear layer is associated with the formation of highly three-dimensional vortex structures. However, even in the latter case the streamline pattern of the attached part of the shear layer still shows laminar-like characteristics, where the typical turbulent spots, originating from wall layer bursts, are obviously absent. Most remarkable, here the line of separation is clearly visible, and three-dimensionality and unsteadiness are found to be much weaker than in the former case. Therefore, this image can hardly be associated with what is commonly referred to as "fully developed turbulent" flow. We note that to our knowledge corresponding measurements for $Re_C > 7.7 \times 10^6$ are currently not available.

Needless to say, the above interpretation of Schewe's data bears some undeniable uncertainties. The present paper, tied in a series of preceding studies on this topic, attempts to shed light on this remarkable finding from a theoretical point of view.

II. Problem Formulation

Here and in the following all lengths, velocities, and the pressure are non-dimensional with, respectively, $\tilde{R}$, $\tilde{U}$, and $\tilde{\varrho}\tilde{U}^2$. Furthermore, let us adopt natural coordinates x, y, according to figure 1 (a). Then the continuity equation is satisfied identically as $u = \partial\psi/\partial y$, $hv = -\partial\psi/\partial x$. Herein $h = 1 + \varkappa(x)\, y$, where the surface curvature $\varkappa(x) = \mathcal{O}(1)$ in general and taken to be positive for a convex body contour; note that $\varkappa \equiv 1$ for the canonical case of a circular cylinder of radius $\tilde{R}$. The time- or, (due to a well-known result of ergod theory) equivalently, Reynolds-averaged Navier–Stokes equations then read (cf. Ref. 13, p. 81)

$$h(\psi_y\partial_x - \psi_x\partial_y)\psi_y - \varkappa\,\psi_x\psi_y = -hp_x - h\langle u'^2\rangle_x - (h^2\langle u'v'\rangle)_y + Re^{-1}h^2(\nabla^2\psi)_y, \tag{2}$$

$$(\psi_x\partial_y - \psi_y\partial_x)(h^{-1}\psi_x) - \varkappa(\psi_y)^2 = -hp_y - (h\langle v'^2\rangle)_y - \langle u'v'\rangle_x + \varkappa\langle u'^2\rangle - Re^{-1}(\nabla^2\psi)_x, \tag{3}$$

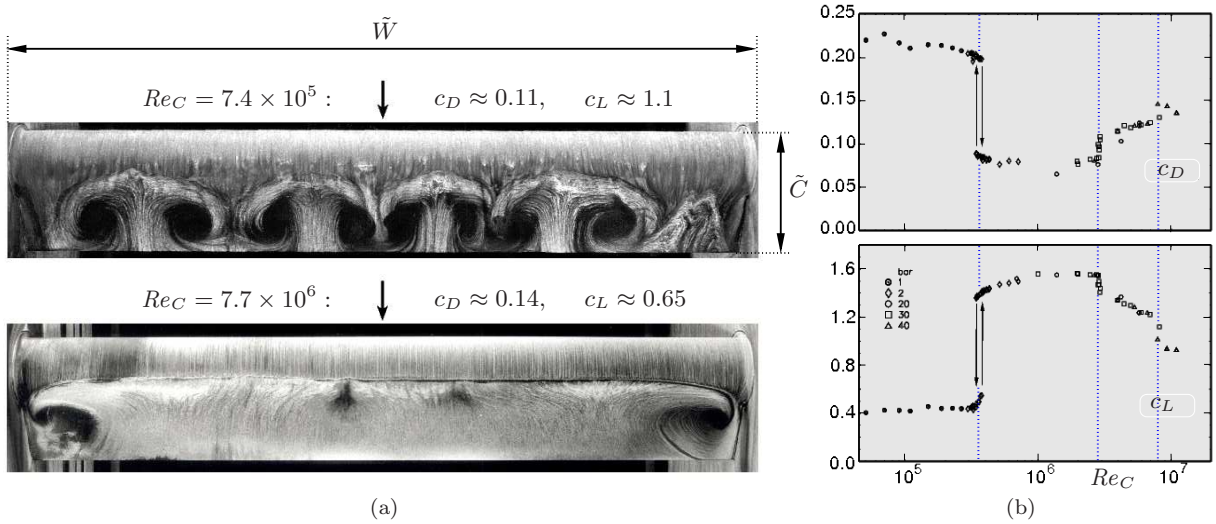

(a) (b)

Figure 2. Measurements on gross separation on the suction side of an airfoil (images by courtesy of and made available by G. Schewe): (a) oil flow film visualizations (vertical arrays indicate flow direction), (b) c_D and c_L versus Re_C, increasing values (in bar) of the suction pressure of the measuring section of the wind tunnel give increasing values of Re_C (logarithmic scale).

where $\nabla^2 = h^{-1}[\partial_x(h^{-1}\partial_x) + \partial_y(h\partial_y)]$ is the Laplacian. The equations of motion (2), (3) are subject to the usual no-slip condition,

$$y = 0: \quad u = v = u' = v' = 0, \tag{4}$$

and the requirement for unperturbed parallel incident flow, having a velocity of magnitude 1, for $y \to \infty$, see figure 1 on page 5. With respect to the subsequent analysis, we tacitly assume that all components $\langle u'^2\rangle$, $\langle u'v'\rangle$, $\langle v'^2\rangle$ of the Reynolds stress tensor are of equal magnitude for given positive values of x and y (common hypothesis of locally isotropic turbulence).

For moderate levels of the turbulence intensity in the BL that emerges in the limit (1) adjacent to the body surface, the latter is seen to be structurally of traditional laminar (i.e. Prandtl-) type.[1] Let us first consider the external flow.

We anticipate the outer expansion[1]

$$[\psi, p] \sim [\psi_0, p_0](x, y; k) + \mathcal{O}(Re^{-1/2}), \quad y = \mathcal{O}(1), \tag{5}$$

such that the impressed external flow described by ψ_0, p_0 is sought in the one-parameter family of Kirchhoff flows, exhibiting free streamlines that confine an (open or closed) cavity and depart at $x = x_{\mathcal{S}}(k)$ from the surface, see figure 1 on page 5. That potential-flow solution is uniquely determined by the non-negative BV parameter k. Specifically, the surface slip velocity $u_e(x;k)$, given by $\partial_y\psi_0$ evaluated for $y = 0$, then exhibits the asymptotic behavior

$$u_e \sim b(k)\, x + \mathcal{O}(x^2) \quad (b > 0), \qquad x \to 0_+, \tag{6}$$

$$u_e/u_{e,\mathcal{S}} \sim 1 + 2k(-s)^{1/2} + 10k^2(-s)/3 + \mathcal{O}\big[(-s)^{3/2}\big], \qquad s = x - x_{\mathcal{S}} \to 0_- . \tag{7}$$

Equation (6) reflects the well-known behavior of the potential flow near a (front) stagnation point, and Eq. (7) states that k measures the strength of the so-called BV singularity taking place at $x = x_{\mathcal{S}}$. Equation (7) stays formally intact even for arbitrarily small values of k if considered as an expansion in the independent double limit $s \to 0_-$, $k \to 0_+$. Note that in the inviscid limit $|\mathbf{u}| \equiv u_{e,\mathcal{S}}(k)$ along $\mathcal{C}$, where $u_{e,\mathcal{S}} = 1$ in case of an open cavity, (according to the definition of $\tilde{U}$), and $u_{e,\mathcal{S}} < 1$ otherwise. Both the derivation of Eq. (7) and the method[3] adopted to obtain global potential-flow solutions, including $u_{e,\mathcal{S}}$ as a function of k, will be presented in a subsequent related study. A brief discussion of the potential flow, based on the numerically obtained solutions, is presented in § IV.A. For the sake of completeness, however, here we mention that the expansion (7) can be calculated from the local behavior of the stream function as $s \to 0_-$, suitably expressed

in polar coordinates,

$$[s, y] = [r\cos\theta, r\sin\theta], \quad r \geq 0, \quad 0 < \theta \leq \pi/2, \tag{8}$$

$$\psi_0/u_{e,\mathcal{S}} \sim r\sin\theta - (4k/3)\, r^{3/2}\cos(3\theta/2) - (5k^2/3)\, r^2\sin(2\theta) + \mathcal{O}(r^{5/2}), \quad k \geq 0, \quad r \to 0. \tag{9}$$

Also, we briefly mention a procedure how the shape $y = y_{\mathcal{C}}$ of the free streamline that departs from the surface in $\mathcal{S}$ can be determined locally from Eq. (9): this expansion formally ceases to be valid near $\theta \sim (4k/3)r^{1/2}$, which gives the leading term in the form

$$y_{\mathcal{C}} \sim (4k/3)s^{3/2} + \mathcal{O}\big(s^{5/2}\big), \quad s \to 0_+ \tag{10}$$

by exploiting the property $\psi_0 = 0$ for $y = y_{\mathcal{C}}$. Note that higher-order terms in Eq. (10) can be calculated recursively in this manner, where those in Eqs. (7) and (9), respectively, are due to the requirement of constant velocity along $\mathcal{C}$.

Concerning the description of the attached BL for $0 \leq x < x_{\mathcal{S}}$, we closely follow Refs. 1, 4. In the inner expansion,

$$[\psi,\, -\langle u'v'\rangle] \sim Re^{-1/2}[\Psi(x, Y; k, T),\, T\Sigma(x, Y; k, T)] + \mathcal{O}(Re^{-1}), \quad Y = Re^{1/2}\, y, \tag{11}$$

the so-called turbulence-level gauge factor T that accounts for the magnitude of the Reynolds stresses (i.e. the turbulence intensity) in the BL is assumed to be a constant of $\mathcal{O}(1)$, in general. Substitution of Eq. (11) into the governing equations (2)–(4) and taking into account Eq. (6) then gives rise to the leading-order BL problem, describing a generic BL that prevails in a transitional (i.e. neither laminar, nor fully turbulent) state,

$$\Psi_Y\Psi_{Yx} - \Psi_x\Psi_{YY} = -p_{0x}(x, 0; k) + T\Sigma_Y + \Psi_{YYY}, \quad p_{0x}(x, 0; k) = -u_e u_{ex} \tag{12}$$

$$Y \to 0: \quad \Psi \to 0, \quad \Psi_Y \to 0, \quad \Sigma = \mathcal{O}(Y^3), \quad Y \to \infty: \quad \Psi_Y - u_e \to 0, \quad \Sigma \to 0, \tag{13}$$

$$x \to 0_+: \quad \Psi/(b^{1/2}x) \to H(b^{1/2}Y), \quad \Sigma = \mathcal{O}(x^2). \tag{14}$$

From the last relationships one infers that Ψ matches with the (from the analysis of laminar flows) well-known Hiemenz solution[13] of the full equations (2)–(4) of motion in the limit (1), which holds near $\mathcal{F}$ where x, y are both of $\mathcal{O}(Re^{-1/2})$: $\psi \sim b^{1/2}x\, H(b^{1/2}Y) + \mathcal{O}(Re^{-1})$, with

$$H'^2 - HH'' = 1 + H''', \quad H(0) = H'(0) = H'(\infty) - 1 = 0. \tag{15}$$

Equations (12)–(15), supplemented with an distribution $u_e(s; k)$, characteristic of the impressed inviscid flow, represent a well-posed initial-boundary value problem for Ψ, provided that Σ is modelled such that it exhibits the required asymptotic properties, expressed in Eqs. (13), (14). Note that the behavior of Σ for $x \to 0_+$ reflects the quite obvious (and by any commonly adopted closure provided) proportionality between the Reynolds stress components and u_e^2, in respect of Eq. (6). In turn, the purely laminar case is simply obtained for $T = 0$. In order to take into account the effect of turbulence, we seek "non-trivial" solutions of Eqs. (12)–(14), i.e. such having $\Sigma \not\equiv 0$ for $T > 0$.

In particular, we subsequently focus on the pronounced turbulent case, associated with the limit $T \to \infty$. To be more precise, it is the primary goal of the present study to elucidate the behavior of these limiting solutions immediately upstream of the BV singularity, expressed by the expansion (7).

Most important, in a flow region close to $\mathcal{F}$ that is characterized by $x = \mathcal{O}(1/T$ and $Y = \mathcal{O}(1)$ in the limit $T \to \infty$, the original problem is seen to be formally fully retained in leading order when u_e is represented by bx, see Eq. (6). However, there the full equations of motion (2), (3) allow for a BL approximation of their streamwise component, Eq. (2), only if $T = o(Re^{1/2})$. This is true as long as $T \ll Re^{1/2}$, which is assumed in the following in agreement with the considerations already outlined in § I.B.

III. Large-T Boundary Layer

In the following, the notation "turbulent BL" is adopted for the flow described by Eqs. (12) and (13) in the limit $T \to \infty$. We now focus on the resulting asymptotic structure of that BL, specifically on its behavior near $\mathcal{S}$. It is well-known that in the purely laminar case ($T = 0$) solutions of the BL problem Eq. (12)–(14) terminate in form of Goldstein singularity for $k > 0$, i.e. if the BV singularity exhibits finite strength;[2,7] a similar situation has been found for $T > 0$.[1] We now investigate this behavior if T takes on arbitrarily large values.

III.A. Initially Attached Flow

In Eq. (12) the Reynolds stress term predominates its viscous counterpart for large values of T if $x = \mathcal{O}(1)$ and Y is sufficiently large, i.e. in the main portion or, equivalently, the fully turbulent region of the BL. Consequently, the problem given by Eqs. (12)–(15) then is singularly perturbed in an (at least) twofold manner,[1] since both shear stress contributions are found to be of the same order of magnitude in two different flow regimes: first, in the so-called transitional-flow region close to $\mathcal{F}$ and sketched in figure 1 on page 5 (b), where rapid laminar-turbulent transition takes place, so that both the suitable streamwise coordinate $X = b^{1/2}\,Tx$ and Y are quantities of $\mathcal{O}(1)$ there; secondly, in the so-called viscous wall layer that is located adjacent to the surface as it evolves from the transitional-flow region, i.e. in the limit $X \to \infty$.

We note that there exists, in addition, a relatively slender so-called superlayer on top of the main region, which is expected to develop from the transitional-flow region also as it accounts for the relatively pronounced outer edge of the turbulent BL and, hence, separates the turbulent motion from the ambient mainly irrotational flow, cf. Ref. 13. However, this overlayer is disregarded here as its existence is rather of minor importance for the understanding of the basic properties the turbulent BL flow which are of interest subsequently. Therefore, by considering Eqs. (12) and the far-field boundary conditions in Eq. (13)), in the following a sharp line $Y = \delta(x; k, T)$, with δ to be determined, will be taken to represent the BL edge with asymptotically sufficient accuracy.

As the process of matching the asymptotic expansions of the flow quantities in those two domains of non-uniformity and with the main layer, respectively, turns out to be essentially governed by the properties of the viscous wall layer, we consider the latter region first. Moreover, a rational description of the turbulent BL, based on minimum of physically motivated assumptions, is advantageously build up from the analysis of that wall region, as the source of the turbulent motion: the turbulent motion originates from its more-or-less universal dynamics that takes place close to the surface;[1] for a more elaborate overview on this topic we refer to Refs. 14–16.

III.A.1. Viscous Wall Layer

The two following basic properties of that region found in the (hypothetical) limiting case $T = Re^{1/2}$ of a fully developed turbulent BL apply unchanged here, cf. Ref. 1:

(A) the time-mean and fluctuating velocity components are of the same order of magnitude, such that $u'v'$ is (at least for most fractions of time) of $\mathcal{O}(u^2)$, and the correlation $\langle u'v'\rangle$ is of $\mathcal{O}(TRe^{-1/2}u^2)$;

(B) for initially firmly attached flow, the imposed pressure gradient, given by $-u_e u_{ex}$, does not enter the leading-order approximation of Eq. (12).

Due to the scaling anticipated in item (A), convective terms in Eq. (12) are negligibly small. As a consequence of the assumption made in item (B), the BL equation then reduces to the well-accepted balance between the wall shear stress and the sum of the Reynolds and the molecular shear to leading order. The latter is commonly believed to be universal, or in perfect "equilibrium", for all types of turbulent wall-bounded shear flows, as it is considered to be independent of x.[1,14–16] The corresponding wall layer scaling fully agrees with that deduced from usually adopted closure schemes for Σ.[4] In turn, we appropriately set

$$\Psi = \Psi^+(x, Y^+; k, T)/T, \quad \Sigma = u_T^2\Sigma^+(x, Y^+; k, T), \quad Y = Tu_T Y^+. \tag{16}$$

Herein, the quantities denoted by the superscript "+" are assumed to be of $\mathcal{O}(1)$. Also, since $-\langle u'v'\rangle$ is seen to be of $\mathcal{O}(TRe^{-1/2}u_T^2)$, the term $Re^{-1/4}T^{1/2}u_T$ is appropriately interpreted as the skin-friction velocity, i.e. the square-root of the wall-shear stress $Re^{1}\partial u/\partial y$ evaluated at $y = 0$, in agreement with item (A) above. Here we conveniently express it by making use of the BL scaling in the form

$$u_T := [\Psi_{YY}(x, 0; k, T)/T]^{1/2}. \tag{17}$$

Then the BL equation (12) are transformed into

$$\partial_{Y^+}\Sigma_t^+ = P^+ + (Tu_T)^{-2}\big[(\partial_x u_T)(\partial_{Y^+}\Psi^+)^2 + u_T(\partial_{Y^+}\Psi^+\,\partial_{xY^+}\Psi^+ - \partial_x\Psi^+\,\partial^2_{Y^+}\Psi^+)\big]. \tag{18}$$

Herein, the sum of the Reynolds and the viscous shear stress, the so-called total shear stress, is written as

$$\Sigma_t^+ := \Sigma^+ + \partial^2_{Y^+}\Psi^+, \tag{19}$$

and P^+ denotes the rescaled imposed pressure gradient,

$$P^+ := -u_e u_{ex}/(T^2 u_T^3) \to 0, \quad T \to \infty. \tag{20}$$

Then the aforementioned stress balance suggests the expansions

$$\mathbf{q}^+ \sim \mathbf{q}^+_{00}(Y^+) + P^+[\mathbf{q}^+_{11}(Y^+) - \gamma^2 \mathbf{q}^+_{12}(Y^+) + \mathcal{O}(\gamma^3)] - \epsilon\,[\mathbf{q}^+_{21}(x, Y^+; k) + \mathcal{O}(\gamma)], \quad \mathbf{q}^+_{ij} := [\Psi^+_{ij}, \Sigma^+_{ij}], \tag{21}$$

provided that the gauge functions are given by

$$\gamma := u_T/u_e \to 0, \quad \epsilon := 1/(T u_T)^4 \to 0, \quad T \to \infty. \tag{22}$$

Note the following three restrictions that lead to the specific form of the expansion (21), where consistency will be shown later: (i) eigensolutions that are due to matching with the flow quantities in the transitional-flow region have been omitted as they do not affect the main results of the subsequent analysis; (ii) it anticipates the relationship

$$\gamma_x = \mathcal{O}(\gamma^2), \tag{23}$$

implied by the dependence of γ on T (derived in § III.A.2 below), as it is assumed that $u_{Tx} = u_{ex}\gamma + \mathcal{O}(\gamma^2)$, such that the remainder terms, indicated by the Landau symbols, turn out to be proportional to γ_x to leading order; (iii) it is based on the aforementioned equilibrium of universal type, associated with the stress balance, which is expected to hold also for $\mathbf{q}_{11}$ and $\mathbf{q}_{12}$, as the x-dependence of terms of $\mathcal{O}(P^+)$ and $\mathcal{O}(P^+\gamma^2)$, respectively, is absorbed into the gauge functions P^+ and γ solely. The idea behind the last assumption becomes clear immediately by inspection of the accordingly expanded BL equation (18), subject to the boundary conditions (12).

Substituting the expansion (21) into Eqs. (18) and (12) then yields, after integration with respect to Y^+ by taking into account the scalings given by Eqs. (16) and (17) and some manipulations,

$$\Sigma^+_{t\,00} = 1, \quad \Sigma^+_{t\,11} = Y^+, \quad \{\Sigma^+_{t\,12},\ \Sigma^+_{t\,21}\} = \int_0^{Y^+} \left\{ \Psi^{+\prime 2}_{00},\ \frac{u_{exx}}{u_e^3}\left[\Psi^{+\prime}_{00}\Psi^{+\prime}_{11} - \Psi^{+\prime\prime}_{00}\Psi^{+}_{11}\right] + 2\frac{u_{ex}^2}{u_e^4}\,\Psi^{+\prime\prime}_{00}\Psi^{+}_{11} \right\} \mathrm{d}\vartheta. \tag{24}$$

Herein, in the integrands Ψ^+_{00} and Ψ^+_{11} are taken to be functions of ϑ. The first two of the relationships (24) represent, respectively, the already mentioned leading-order equilibrium between the total shear and the wall shear stress and the dominant effect of the imposed pressure gradient on the wall layer flow. These relationships initiate the infinite sequence of equations that determine $\Sigma^+_{t\,ij}$. That is, they can be solved hierarchically to predict Ψ^+_{ij} as functions of x, Y^+, and k, subject to the no-slip conditions $\Psi^+_{ij} = \partial_{Y^+}\Psi^+_{ij} = 0$ for $Y^+ = 0$, once the conditions of matching with the fully turbulent flow for $Y^+ \to \infty$ are known and a suitable closure for Σ^+ is provided. In addition, the near-wall behavior can be elucidated by assuming that

$$\Sigma^+_{ij} \sim \varepsilon_{ij} Y^{+3} + \cdots \quad (\varepsilon_{00} > 0), \quad Y^+ \to 0, \tag{25}$$

in agreement with Eq. (13). Hence, this relation indicates that

$$[\Psi^+_{00}, \Psi^+_{11}, \Psi^+_{ij}] \sim [Y^{+2}/2 - \varepsilon_{00} Y^{+5}/20,\ Y^{+3}/6 - \varepsilon_{11} Y^{+5}/20,\ -\varepsilon_{ij} Y^{+5}/20] + \cdots \quad (i+j > 2), \quad Y^+ \to 0, \tag{26}$$

since the effects of wall shear stress and the pressure gradient in the expansion (21) are subsumed into the dominant "equilibrium" terms $\mathbf{q}^+_{00}$ and $\mathbf{q}^+_{11}$, respectively.

The behavior of the leading-order quantities Σ^+_{00}, Ψ^+_{00} on top of the viscous wall layer is crucial for the subsequent analysis. First, since the viscous contribution, $\Psi^{+\prime}_{00}$, to $\Sigma^+_{t\,00}$ is presumed to vanish there,

$$\Sigma^+_{00} \to 1, \quad Y^+ \to \infty. \tag{27}$$

Secondly, we conclude the wall layer analysis by introducing the celebrated logarithmic law of the wall, which is commonly believed to hold for fully developed turbulent wall-bounded flow flow and has been introduced by adopting asymptotic reasoning in the seminal paper by Mellor:[5] there are convincing reasons to believe that the behavior

$$\Psi^{+\prime}_{00} \sim \kappa^{-1} \ln Y^+ + B^+, \quad Y^+ \to \infty, \tag{28}$$

is typical for the universal character of the time-averaged flow in the near-wall region.[1,4,14–17] Most important, integration of the first of the relationships (24) by employing any realistic closure model for the turbulent stress function Σ^+ then is assumed to reproduce the presently accepted empirical values[18] $\kappa \approx 0.384$ and $B^+ \approx 4.1$, which refer to a perfectly smooth surface.

We will see in the following that the adoption of the logarithmic law (28) indeed implies the initial assumption (B) or, equivalently, the limits expressed in Eqs. (20) and (22).

III.A.2. Outer Defect Layer

As has already been outlined in Ref. 1, see also § I, § II, and figure 1 on page 5 (b), the downstream evolution of the transitional BL for $X \to \infty$ exhibits a small streamwise velocity defect with respect to the external flow in the outer main portion of the BL. Accordingly, the Reynolds stress function Σ there becomes small, too.

Let the velocity defect and Σ be measured by the two gauge functions $\chi(T)$ and $\sigma(T)$ in the form

$$[\eta - \Psi/(u_e\delta),\ \Sigma/(u_e^2\sigma)] = \chi\,[F, S], \quad (\chi, \sigma) \to (0, 0), \quad T \to \infty. \tag{29}$$

From inspection of Eq. (12) one then readily infers that $\delta = \mathcal{O}(T\sigma)$. In turn, a suitable outer-layer coordinate η is introduced by setting

$$Y = \delta\eta, \quad \delta := T\sigma\Delta(x; k, T). \tag{30}$$

Then the flow quantities are expected to have expansions of the form

$$\big\{[F, S],\ \Delta\big\} \sim \chi\mathbf{q}_1 + \chi^2\mathbf{q}_2 + \mathcal{O}(\chi^3), \quad \mathbf{q}_i := \big\{[F_i, S_i](x, \eta; k),\ \Delta_i(x; k)\big\}. \tag{31}$$

Again, here we have disregarded the occurrence of eigensolutions that result from matching the main layer with the transitional-flow region, without loss of generality.

With respect to the subsequent investigation, it is sufficient to inspect the (homogeneous) leading-order equation only, which exhibits linearized convective terms. It is obtained by inserting Eq. (31) into Eq. (12), subsequent integration with respect to η, and imposing the proper boundary condition $F_1(x, 0) = 0$,

$$u_e^2(u_e\Delta_1)_x\eta F_{1\eta} - (u_e^3\Delta_1 F_1)_x = u_e^3(S_1 - S_{1,b}), \quad S_{1,b} := S_1(x, 0; k). \tag{32}$$

We first consider the specific role of matching the flow in the main layer with that in the transitional region,[1] which requires that $[F_1, S_1](0, \eta; k)$ exists, where $F_1(0, \eta; k) > 0$ for $0 < \eta \le 1$, $S_1(0, \eta; k) > 0$ for $0 < \eta < 1$, and $\Delta \to 0$ as $x \to 0_+$. Since patching the flow at the BL edge is only possible if $F_{1\eta}(x, 1; k) = S_1(x, 1; k) = 0$, the shear stress term S_1 in Eq. (32) then is seen to enter the least-degenerate form that equation takes on in this limit; otherwise, the resulting problem for $[F_1, S_1](0, \eta; k)$ would have no solution. By taking into account Eq. (6), one consequently finds that all terms of Eq. (32) are retained in the limit $x \to 0_+$ and, interestingly, the dependence on k disappears. As a remarkable finding, the solution of Eq. (32) that holds for $x = 0$ admits an universal form,

$$[F_1, S_1] \sim [G, J](\eta) + \mathcal{O}(x), \quad \Delta_1 \sim \Xi x + \mathcal{O}(x^2) \quad (\Xi > 0), \quad x \to 0_+. \tag{33}$$

These considerations also show why the case $S_{1,b} = 0$ is to be excluded: it would imply that (the for $x > 0$ strictly positive) quantity $u_e^3\Delta_1 F_1(x, 1; k)$ is independent of x and, thus, yield the contradiction $\Delta_1 F_1(x, 1; k) = \mathcal{O}(x^{-3})$ as $x \to 0_+$. Most important, then the matching conditions (27) and (28) allow for a direct match of the wall layer with the outer main layer. In turn, both the parameters χ and σ are conveniently identified formally with γ, cf. figure 1 on page 5 (b), leaving Eq. (32) unchanged, when we again anticipate the estimate (23). As a result, $S_{1,b} = 1$, and Eq. (32) is supplemented with the boundary and matching conditions[1]

$$\eta \to 0: \quad F_1 \to 0, \quad F_{1\eta} \sim -\kappa^{-1}\ln\eta + B_1(x; k), \quad S_1 \to 1, \qquad \eta = 1: \quad F_{1\eta} = F_{1\eta\eta} = S_1 = 0. \tag{34}$$

Herein, the (positive) function $B_1(x; k)$ is considered as part of the solution for $F_1(x, \eta; k)$, and the requirement $S_1 = 0$ for $\eta = 1$ is associated with vanishing vorticity, expressed through $u_T F_{1\eta\eta}/\delta$, at the BL edge. Also, it is useful to state the aforementioned relationship that follows from evaluation of Eq. (32) for $\eta = 1$,

$$\big[(u_e^3\Delta_1)(x; k)\,F_1(x, 1; k)\big]_x = u_e^3(x; k), \quad (u_e^3\Delta_1)(x; k)\,F_1(x, 1; k) = \int_0^x u_e^{-3}(\vartheta; k)\,\mathrm{d}\vartheta. \tag{35}$$

The latter of these relationships represents the integral momentum balance for the small-defect description of turbulent BL flow,[13] which is obtained by making use of Eq. (33).

The knowledge of the universal functions G, J then completes Eqs. (32) and (34) to an initial-boundary value problem for F_1, S_1 for $x \ge 0$. In principle, this can be solved by means of downstream integration if an asymptotically correct closure for S is provided that accounts for the logarithmic singularity of $F_{1\eta}$, see

Eq. (34). Evaluation of Eqs. (32) and (34) for $x \to 0_+$ shows that G, J are self-similar solutions of these equations,[1]

$$2\Xi[\eta G' - 2G] = J - 1, \quad \Xi = 1/[4\,G(1)], \tag{36}$$

$$\eta \to 0: \quad G \to 0, \quad G' \sim -\kappa^{-1} \ln \eta + D, \quad G(1) = J(1) = 0. \tag{37}$$

By considering Eq. (37), one finds that $D = \lim_{x\to 0} B_1(x;k)$ and, thus, not known in advance. Interestingly, the universal boundary value problem posed by Eqs. (36) and (37) can be interpreted as the turbulent counterpart to the Hiemenz or laminar stagnating-flow problem (15). Note that the transitional flow "connects" the Hiemenz flow, serving as an initial condition for $X = 0$, and its limiting downstream form, given by Eqs. (36) and (37) and obtained for $X \to \infty$.[1]

Finally, matching of the streamwise velocity, Ψ_Y, completes the leading-order analysis as it reveals the yet missing dependence of γ on T and the relationship (23) in terms of the "skin-friction law"

$$\gamma \sim \kappa\tau\,[1-\tau(2\ln\tau+E)+4\tau^2\ln\tau\,(\ln\tau+E+1)+\mathcal{O}(\tau^2)], \quad E := \kappa(B^+ + B_1) + \ln(\kappa^2 u_e \Delta_1), \quad \tau := \frac{1}{2\,\ln T}. \tag{38}$$

This relationship is consistent with the assumption (B) made at the beginning of § III.A.1 as it justifies the limits expressed in Eq. (20) and, in turn, Eq. (22), and the estimate (23). We remark that the remainder terms in the expansion (38), indicated by the Landau symbol, are already affected by terms of $\mathcal{O}(\gamma^2)$ in the expansion (31). Also, note that the viscous stress term Ψ_{YY}, entering Eq. (12), is asymptotically given by $-u_e F_{1\eta\eta}/(T\Delta_1)$.

The analysis carried out so far confirms that the investigation of the large-T BL can essentially be traced back to that of a conventional fully developed turbulent BL[1] when T is formally replaced by its theoretical upper bound $Re^{1/2}$, which can never be reached here, however.

III.B. Boundary Layer Structure near Separation

First, let us refer to the sketch in figure 3 that depicts the asymptotic splitting of the BL deduced in the subsequent investigation.

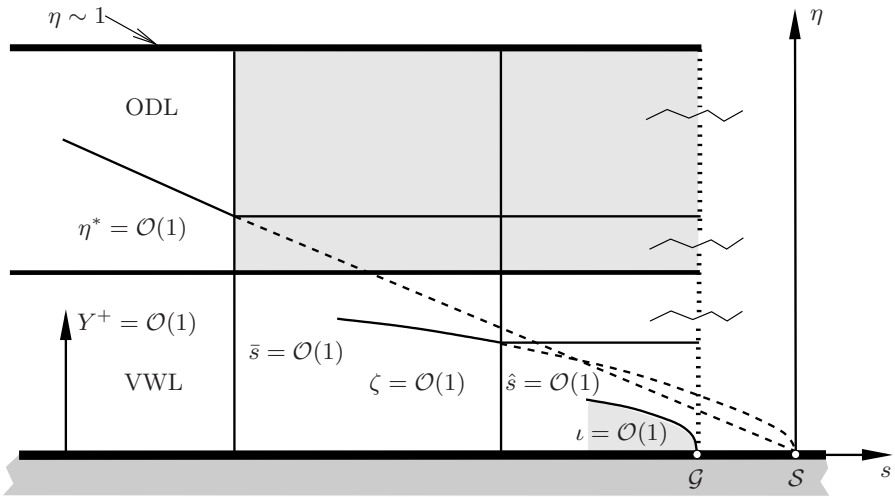

Figure 3. Asymptotic splitting of BL flow near $x = x_S$ (schematic), light-shaded regions not discussed explicitly in the text (Goldstein region and passive small-defect regions near $\mathcal{G}$), broken lines confine fictitious extension of respective regions, dotted vertical line indicates abrupt breakdown of flow description at $\mathcal{G}$.

The matching principle states that an asymptotically correct description of the BL flow in the limit $T \to \infty$ is initiated by seeking a solution of Eqs. (36), (37) and, in the following, of Eq. (32) by means of downstream integration. Therefore, we first envisage the behavior of its solution F_1, S_1 as $s \to 0_-$.

III.B.1. Outer Defect Layer

The local behavior of the small-defect flow near separation has already been accounted for briefly in Ref. 6. Here we present the analysis in a more precise manner, which, amongst others, accounts for the impact of

higher-order terms in the resulting expansion, in close connection with the logarithmic behavior required by Eq. (34).

Inspection of Eqs. (7) and (the second relationship in Eq.) (35) shows that the product $\Delta_1 F_1(x,1;k)$ is bounded in the limit $s \to 0_-$. Since $F_1 > 0$ for $\eta > 0$, the second term in Eq. (32) then is a quantity of $\mathcal{O}(1)$. Furthermore, physically motivated reasoning, substantiated by inspection of any commonly employed (outer-layer) turbulence closure,[1,6] strongly suggests that

$$S = \mathcal{O}\big(F_{1_{\eta\eta}}^2\big). \tag{39}$$

In turn, if one assumes (the rather unexpected case) $S_1 \to 0$ as $s \to 0_-$ it is readily found that all terms apart from $u_e^3 S_1$ will enter the leading-order balance of Eq. (32). However, for the same reason explained for the case $x \to 0_+$ treated above, the resulting equation determining F_1 for $S_1 \to 0$ is inconsistent with the boundary conditions (34). Therefore, we are left with the two remaining possibilities $S_1 \to \infty$ or $S_1 = \mathcal{O}(1)$. In the first case Eq. (32) would reduce to a balance between the left-most term and $u_e^3 S_1$ in leading order (accompanied by the emergence of a sublayer, located between the viscous wall and the main layer, due to the apparent inconsistency of the boundary conditions (34) with that balance). However, Eq. (39) then implies $F_1 \to \infty$ and, consequently, $\Delta_1 \to 0_+$ as $s \to 0_-$. The last finding not only is felt to misinterpret the physical mechanism of separation, but, more drastically, causes the first term in Eq. (32) to have negative sign and, therefore, a contradiction.

As a preliminary (and rather startling) result, the flow quantities assume finite limits when the external flow encounters the BV singularity. We then appropriately expand

$$\big\{[F_1, S_1], \Delta_1\big\} \sim \mathbf{q}_{10} + \lambda'(s)\,\mathbf{q}_{11} + (-s)^{1/2}\mathbf{q}_{12} + (-s)\mathbf{q}_{13} + \mathcal{O}(\lambda), \quad \mathbf{q}_{1j} = \big\{[F_{1j}, S_{1j}](\eta;k), \Delta_{1j}(k)\big\}. \tag{40}$$

where $\lambda(s) \to 0$, $\lambda'(s) \to 0$, and $s \to 0_-$. Note that $F_{10} > 0$ and that S_{10} is non-negative; both these quantities are part of the global solution of Eqs. (32) and (34). In the expansion (40) the term $\mathbf{q}_{11}$ refers to an eigensolution of, for the time being, unknown strength λ, and the contributions $\mathbf{q}_{1j}$, $j > 1$, primarily account for the local behavior (7) of u_e and the coupling between F_1 and Δ_1 in Eq. (32); the flow is seen to be inviscid for terms smaller than of $\mathcal{O}(-s)$. Inserting the expansion (40) into Eq. (32) yields the equations determining $\mathbf{q}_{11}$ and $\mathbf{q}_{12}$ as

$$F_{11} = (\Delta_{11}/\Delta_{10})(\eta F_{10_\eta} - F_{10}), \quad F_{12} = (2k + \Delta_{12}/\Delta_{10})\,\eta F_{10_\eta} - (6k + \Delta_{12}/\Delta_{10})\,F_{10} + \cdots. \tag{41}$$

Herein, the dots indicate possible inhomogeneities due to a coupling between F_{11} and Δ_{11}, enforced by Eq. (32). However, the solution for F_{11} does not satisfy the condition of vanishing vorticity, given by $F_{11_{\eta\eta}}$, for $\eta = 1$ according to Eq. (34) (except for unlikely circumstances where $(\partial_\eta^3 F_{10})(1;k) = 0$). Consequently, we assume $\lambda = 0$, so that Eq. (40) reduces to an expansion in terms of integer powers of $(-s)^{1/2}$. Note that $(F_{12_\eta})(1;k) = 0$, and adopting the aforementioned condition for F_{12} in Eq. (41) then yields the solvability conditions

$$F_{12} = -4kF_{10}, \quad \Delta_{12} = -2k\Delta_{10}. \tag{42}$$

In principle, proceeding in this fashion gives $\mathbf{q}_{1j}$, $j > 1$, where the boundary conditions for $\eta = 1$ can be fulfilled solely by exploiting the convective operator in Eq. (32).

Next, we stipulate that

$$F_{10} \sim F_{10,b}(\eta) := [-\kappa^{-1}(\ln\eta - 1) + B_{1,\mathcal{S}}]\eta, \quad B_{1,\mathcal{S}} := B_1(x_\mathcal{S};k), \quad S_{10} \to 1, \quad \eta \to 0, \tag{43}$$

in accordance with the requirements of matching with the near-wall flow given in Eq. (34). Unfortunately, F_{12_η} then will also exhibit a logarithmic singularity, cf. Eq. (42), which clearly violates the original near-wall condition for F_{1_η} (and, in turn, for S_1). This inconsistency can only be resolved by the introduction of a sublayer of (the initially unknown) relative thickness $\Delta^*(s)$. The therewith suggested stretching transformation

$$[F_1/\Delta^*(s),\, S_1] = [F^*,\, S^*](s, \eta^*; k) = \mathcal{O}(1), \quad \eta = \Delta^*(s)\,\eta^*, \quad \Delta^* \to 0_-, \quad s \to 0_-, \tag{44}$$

casts Eq. (32) into the form

$$u_e^2(u_e\Delta_1\Delta^*)_s\,\eta^* F^{**}_{\eta} - (u_e^3\Delta_1\Delta^* F^*)_s = u_e^3(S^* - 1). \tag{45}$$

Substitution of the appropriate expansions

$$[F^*,\, S^*] \sim [-\eta^*\kappa^{-1}\ln\Delta^* + F_{10,b}(\eta^*),\, 1] + (-s)^{1/2}\left[4k\,\eta^*\kappa^{-1}\ln\Delta^* + F_1^*(\eta^*;k),\, S_1^*(\eta^*;k)\right] + \cdots, \tag{46}$$

into Eq. (45) and taking into account Eqs. (7) and the second of the relationships (42) then shows that the least-degenerate form of Eq. (45) reduces to a balance to be aimed at to determine F_1^* and S_1^*,

$$2k(-s)^{-1}\Delta^* F_{10,b}(\eta^*) - 4k\,\eta^*\kappa^{-1}\Delta_s^* + \Delta_s^*\,\eta^* F_{1\eta^*}^* - [\Delta_s^* - (-2s)^{-1}\Delta^*]F_1^* + \mathcal{O}\big[(-s)^{-1/2}\Delta^*\ln\Delta^*\big] \sim S_1^*. \tag{47}$$

This suitably reduced equation not only proves consistency with the assumed behavior (43). Most important, it fixes that

$$2k\eta^*[B_{1,\mathcal{S}} + \kappa^{-1}(3 - \ln\eta^*)] - \eta^* F_{1\eta^*}^* + (3/2)F_1^* = S_1^*, \quad \Delta^* = -s, \tag{48}$$

in order to allow for a solution $[F_1^*, S_1^*](\eta^*;k)$ that satisfies the required matching and boundary conditions

$$\eta^* \to \infty: \quad F_{1\eta^*}^* \sim a_0^*\eta^{*1/2} + 4k(\kappa^{-1}\ln\eta^* - B_{1,\mathcal{S}}) + \mathcal{O}\big(\eta^{*-1/2}\big), \quad \eta^* = 0: \quad F_1^* = S_1^* = 0 \quad [F_1^{*\prime} = \mathcal{O}(1)]. \tag{49}$$

Herein, the condition for $\eta^* \to \infty$ follows from the asymptotic behavior of Eq. (48) and the first of the relationships (42). According to Eq. (43), matching with the main region where $\eta = \mathcal{O}(1)$ yields

$$F_{10\eta} \sim F_{10,b}{}'(\eta) + a_0^*\eta^{1/2} + \cdots \quad (a_0^* > 0), \quad \eta \to 0. \tag{50}$$

Herein, a_0^* is determined by the global solution of Eqs. (32) and (34). Interestingly, an analogous square-root behavior of the leading-order velocity profile is well-known to hold (albeit in the context of a quite different asymptotic framework) for a turbulent BL on the verge of marginal separation.[17,19]

For a specific closure in agreement with Eq. (39), like the mixing-length-based formulation

$$S^* := (\kappa\eta^*\partial_{\eta^*}^2 F^*)^2, \quad S_1^* = 2\kappa\eta^*\partial_{\eta^*}^2 F_1^*, \tag{51}$$

which is commonly believed to hold on top of the viscous wall layer.[13] The second relationship in Eq. (51) then follows from linearization about the terminal velocity profile, F_{10}', by using Eq. (43) and Eq. (46). In turn, one recognizes that only the conditions for $\eta^* = 0$ in Eq. (49) represent true boundary conditions. Those for $\eta^* \to \infty$ are seen to be satisfied identically. By adopting the simple model given by Eq. (51), evaluation of Eqs. (48) subject to the boundary conditions (49) for $\eta^* \to 0$ yields

$$F_1^* \sim K\eta^* - k/(2\kappa^2)\,\eta^{*2}\ln\eta^* + [K/(8\kappa) + k(9 + 2\kappa B_{1,\mathcal{S}})/(4\kappa^2)]\,\eta^{*2} + \mathcal{O}\big(\eta^{*3}\ln\eta^*\big), \quad K := F_{1\eta^*}^*(0;k). \tag{52}$$

In fact, the velocity defect at the base of the defect layer is increased by an amount of $\mathcal{O}[(-s)^{1/2}\ln(-s)]$ as it follows from Eqs. (34) and (46) that

$$B_1 \sim B_{1,\mathcal{S}} + (-s)^{1/2}[(4k/\kappa)\ln(-s) + K] + \mathcal{O}[(-s)\ln(-s)]. \tag{53}$$

In passing we mention that a closed solution of Eqs. (48) and (49), based on the rather simple but asymptotically correct closure (51), is given by[20]

$$F_1^* = \check{\eta}\,\mathrm{e}^{-\check{\eta}/4}\left[\frac{a_0^*\,\pi^{1/2}}{(2\kappa^{-1})^{3/2}}\left[(\check{\eta}+1)I_1\Big(\frac{\check{\eta}}{4}\Big) + (\check{\eta}+3)I_0\Big(\frac{\check{\eta}}{4}\Big)\right] - \frac{4k}{3}\left[(\check{\eta}+1)K_1\Big(\frac{\check{\eta}}{4}\Big) - (\check{\eta}+3)K_0\Big(\frac{\check{\eta}}{4}\Big)\right]\right] + F_{1,p}^*,$$
$$F_{1,p}^* = (16k/3) - 4k\eta^*[B_{1,\mathcal{S}} + \kappa^{-1}(1 - \ln\eta^*)], \quad \check{\eta} := \kappa^{-1}\eta^*. \tag{54}$$

Inspection of the scalings (16) and (30) indicates a collapse of the sublayer where $\eta^* = \mathcal{O}(1)$ with the viscous wall layer when $-s = \mathcal{O}[(T\gamma)^{-2}]$. However, we will see subsequently that this scenario is prevented by the asymptotic structure of the wall layer as $s \to 0_-$, which assigns the outer layer an essentially passive role. Hence, we conclude the analysis of the analysis of the outer defect layer by emphasizing the basic result that the primary expansion (31) is seen to be uniformly valid in the (independent) double limit $s \to 0_-$, $\chi = \gamma \to 0$.

III.B.2. Viscous Wall Layer

The more demanding part of the analysis concerns the near-wall flow. Here both the pressure gradient and convective term are found to be initially negligibly small, cf. Eqs. (20)–(22), but inevitably provide a leading-order effect near separation where the gradients with respect to x become arbitrarily large, as a consequence of the behavior (7). Let us first demonstrate how they come into play in a rather subtle manner as $s \to 0_-$.

In the latter limit expansion (21) remains valid and, simultaneously, accounts for the sequence (24) as long as $\mathbf{q}_{11}$ enters the equation determining $\mathbf{q}_{21}$ as a quantity that is regarded as known already. In other words, as long as this condition holds, each term in Eqs. (21) and (24) can be expanded into integer powers of $(-s)^{1/2}$, according to Eq. (7). This is accomplished by expanding the quantity E in Eq. (38) according to Eq. (53) and keeping T fixed, giving

$$\gamma \sim \gamma_0 + \mathcal{O}[\tau^2(-s)^{1/2}\ln(-s)], \quad s \to 0_-, \quad \gamma_0 := \lim_{s\to 0_-}\gamma \sim \kappa\tau\,[1 - 2\tau\ln\tau + \mathcal{O}(\tau)], \tag{55}$$

so that $\gamma_x = \mathcal{O}[\gamma_0^2/(-s)^{1/2}]$ now suitably replaces the relationship (23). Substituting these expressions into the expansion (21) then results in an uniformly valid expansion holding in the (independent) double limit $s \to 0_-$, $T \to \infty$, which ceases to be valid when $\epsilon\,\mathbf{q}_{21}^+ = \mathcal{O}(P^+)$. In the expression for $\Sigma_{t\,21}^+$ in Eq. (24) the first term then predominates the second as $s \to 0_-$; hence, the breakdown occurs when $u_{exx}/u_{ex} \sim 1/(-2s) = \mathcal{O}(T^2\gamma)$, i.e. where $-s = \mathcal{O}[1/(T^2\gamma)]$. Note that Eqs. (38) and (55) then yield

$$\gamma \sim \gamma_0 + \mathcal{O}(\tau^{3/2}\ln T/T), \quad \gamma_x = \mathcal{O}\big(\gamma_0^{5/2} T\ln T\big). \tag{56}$$

We now concentrate on this distinguished limit by introducing a suitable streamwise coordinate $\bar{s} = \mathcal{O}(1)$,

$$s = \bar{s}/(T^2 u_{T0}), \quad u_{T0} := \gamma_0\, u_{e,\mathcal{S}}. \tag{57}$$

We then obtain from Eqs. (20) and (55)–(57)

$$P^+ \sim \pi^+(-\bar{s})^{-1/2}\,[1 + \mathcal{O}(\tau^{1/2}/T)], \quad \pi^+ := k/[T\gamma_0^{5/2}u_{e,\mathcal{S}}]. \tag{58}$$

In the expansion of Ψ^+, Σ^+, resulting from inspection of Eq. (18), then only the first two terms are of interest for the subsequent analysis,

$$[\Psi^+, \Sigma^+] \sim [\Psi_{00}^+, \Sigma_{00}^+](Y^+) + \pi^+\big\{[\bar{\Psi}^+, \bar{\Sigma}^+](\bar{s}, Y^+) + \mathcal{O}(\gamma_0^2)\big\}, \quad T \to \infty. \tag{59}$$

Herein, $\bar{\Psi}^+$, $\bar{\Sigma}^+$ are quantities of $\mathcal{O}(1)$. Inserting Eq. (59) into the BL equation (18) and expanding gives rise to a linear initial-boundary value problem for these quantities,

$$\partial_{Y^+}\bar{\Sigma}^+ + \partial_{Y^+}^3\bar{\Psi}^+ = (-\bar{s})^{-1/2} + \Psi_{00}^{+\prime}\partial_{\bar{s}Y^+}\bar{\Psi}^+ - \Psi_{00}^{+\prime\prime}\partial_x\bar{\Psi}^+, \quad \Psi_{00}^+ = \Psi_{00}^+(Y^+), \tag{60}$$

$$Y^+ = 0: \quad \bar{\Psi}^+ = \partial_{Y^+}\bar{\Psi}^+ (= \bar{\Sigma}^+) = 0, \quad \bar{s} \to -\infty: \quad [\bar{\Psi}^+, \bar{\Sigma}^+] \sim (-\bar{s})^{-1/2}\,[\Psi_{11}^+, \Sigma_{11}^+]\,\big(+\mathcal{O}\big[|\bar{s}|^{-3/2}\big]\big). \tag{61}$$

Equations (60) and (61) have to be supplemented with appropriate matching conditions for $Y^+ \to \infty$. These provide a match with the outer defect layer as they follow from the matching conditions to be imposed on the equations for $\Sigma_{t\,11}^+$ and $\Sigma_{t\,21}^+$ for $-s = \mathcal{O}(1)$, see Eq. (24). Note that they depend on the higher-order properties of any specific closure for Σ^+ that accounts for the leading-order overlap behavior given by (27) and (28). For the present investigation, however, it is only relevant to consider the behavior of the solution to the problem posed by Eqs. (60) and (61) in the limit $\bar{s} \to 0_-$. We stress that the understanding of the BL flow near separation is essentially provided by the local interplay between the two terms quoted in the expansion (59) in the double limit $\bar{s} \to 0_-$, $Y^+ \to 0$. Hence, the following analysis shows close resemblance with that of the purely laminar case, where we refer to the study by Messiter and Enlow[21] and the synopsis presented in Ref. 2: the only striking difference is that here $k = \mathcal{O}(1)$ and the problem for perturbation stream function $\bar{\Psi}^+$ accounts for the relatively weak convective terms in the strongly viscosity-affected near-wall flow region, whereas in the laminar case the corresponding perturbation is due to an asymptotically weak BV singularity, giving $k = \mathcal{O}(Re^{-1/16})$, but convection predominates throughout.

It is obvious that the shear stress terms do not enter the leading-order balance Eqs. (60) reduces to in the limit $\bar{s} \to 0_-$. Then the behavior of $\bar{\Psi}^+$ for $\bar{s} \to 0_-$ and $Y^+ = \mathcal{O}(1)$ in its most general form is found in the form

$$\bar{\Psi}^+ \sim \bar{\Psi}_0^+(Y^+) + \alpha(\bar{s})\,\Psi_{00}^{+\prime}(Y^+) - 2(-\bar{s})^{1/2}\,\Psi_{00}^{+\prime}(Y^+)\left[\frac{1}{Y^+} + \int_0^{Y^+}\left(\frac{1}{\vartheta^2} - \frac{1}{[\Psi_{00}^{+\prime}(\vartheta)]^2}\right)\mathrm{d}\vartheta\right] + \mathcal{O}(-\bar{s}), \tag{62}$$

where both the contribution of $\mathcal{O}(1)$, $\bar{\Psi}_1^+$, and the gauge function $\alpha(\bar{s})$ that accounts for the occurrence of eigensolutions are a priori unknown. However, the local solution given in Eq. (62) does not satisfy the no-slip condition (61). Therefore, a sublayer has to be introduced where the viscous stress term plays a dominant role. From gives $Y^+ = \mathcal{O}[(-s)^{1/3}]$. Moreover, eqs

$$\Psi_{00}^+ \sim (-\bar{s})^{2/3}\zeta^2/2 + \mathcal{O}[(-\bar{s})^{5/3}], \quad \bar{\Psi}_1^+ \sim (-\bar{s})^{1/2} f(\zeta) + \mathcal{O}\big[(-\bar{s})^{3/2}\big], \quad Y^+ = (-\bar{s})^{1/3}\zeta, \quad \zeta = \mathcal{O}(1). \tag{63}$$

Substituting this expansion into Eqs. (60) and (61) yields

$$\zeta^2 f''/3 - \zeta f'/2 + f/2 = -1 + f''', \quad f(0) = f'(0) = 0. \tag{64}$$

The solution to this problem that exhibits sub-exponential growth for $\zeta \to \infty$ can be expressed through confluent hypergeometric functions by adopting standard techniques:[20]

$$f(\zeta) = -2\zeta \int_0^\zeta \big[\Lambda\, M(\tfrac{1}{6}, \tfrac{5}{3}, \vartheta^3/9) + [M(-\tfrac{1}{2}, \tfrac{1}{3}, \vartheta^3/9) - 1]/\vartheta^2\big]\, \mathrm{d}\vartheta, \quad \Lambda := \frac{\Gamma(\frac{1}{3})\,\Gamma(\frac{7}{6})}{3^{1/3}\,\pi^{1/2}\,\Gamma(\frac{5}{3})} \doteq 1.0770, \tag{65}$$

$$f \sim -a_0\zeta^{3/2} + a_1\zeta - 2 + \mathcal{O}\big(\zeta^{-3/2}\big), \quad \zeta \to \infty, \quad [a_0, a_1] := \left[\frac{4\,\Gamma(\frac{1}{6})}{3\,\Gamma(\frac{2}{3})},\, 48^{1/3}\,\Gamma(\tfrac{2}{3})\right] \doteq [5.4809, 4.9212]. \tag{66}$$

Note the pronounced increase of the resulting negative perturbation in the resulting expansion of the wall shear:

$$Y^+ = 0: \quad \partial_{Y^+}^2 \Psi^+ \sim 1 - 2\Lambda\,\pi^+(-\bar{s})^{-1/6} + \cdots, \quad \bar{s} \to 0_-, \quad T \to \infty. \tag{67}$$

Finally, matching the region where $\zeta = \mathcal{O}(1)$ and the main portion of the viscous wall layer, where $Y^+ = \mathcal{O}(1)$, then gives

$$\bar{\Psi}_0^+ \sim -a_0 Y^{+3/2}, \quad Y^+ \to 0, \quad \alpha \sim a_1(-\bar{s})^{1/6}, \quad \bar{s} \to 0_-. \tag{68}$$

That is, $\bar{\Psi}^+$ is bounded for $\bar{s} \to 0_-$, and, accordingly, the contribution to the Reynolds stress, $\bar{\Sigma}^+$, assumes a finite limit,

$$\bar{\Sigma}^+ \sim \bar{\Sigma}_0^+(Y^+) + (-\bar{s})^{1/6}\bar{\Sigma}_1^+(Y^+) + \cdots, \quad \bar{s} \to 0_-. \tag{69}$$

Remarkably, the terminal structure of the problem (60), (61) in the limit $\bar{s} \to 0_-$ is found to be universal, i.e. independent of the specific form of the (exponentially decreasing) eigensolutions for $\bar{s} \to -\infty$, which trigger a non-zero wall shear contribution, $(\partial_{Y^+}^2 \bar{\Psi}^+)(\bar{s}, Y^+ = 0) \not\equiv 0$, that results in the perturbation given in the expansion (67). That is, the existence of these eigensolutions, not considered here, is crucial for the asymptotic structure of the flow as $\bar{s} \to 0_-$.

We also note that the expansion (40) remains essentially intact, as a consequence of the logarithmic behavior (28), in the narrow region where $\bar{s} = \mathcal{O}(1)$, if γ is replaced by γ_0. Moreover, it will turn out in § III.B.3 below that the flow in the outer main layer is virtually unaffected by the wall layer flow for $1/T \ll x < x_{\mathcal{G}}$ throughout, i.e. even for the terminal distinguished limit $\bar{s} \to 0_-$ as $T \to \infty$.

III.B.3. Nonlinear Breakdown

Most important, a further breakdown of the hitherto existing asymptotic structure is encountered when $\pi^+\bar{\Psi}_1^+ = \mathcal{O}(\Psi_{00}^+)$ or, by inspection of Eqs. (59), (63), or (67), for $(-\bar{s})^{1/6} = \mathcal{O}(\pi^+)$, thus, giving rise to a new sublayer. Therefore, this flow regime is conveniently described by assuming that the streamwise coordinate $\hat{s}$, defined by

$$\bar{s} = \pi^{+6}\hat{s}, \tag{70}$$

is a quantity of $\mathcal{O}(1)$. Let us first consider the main portion of the wall layer, namely the so-called core region, where both Y^+ and $\hat{s}$ are quantities of $\mathcal{O}(1)$.

Note that the pressure gradient term P^+ then has increased in magnitude from $\mathcal{O}(\pi^+)$, see Eq. (58), to $\mathcal{O}(1/\pi^{+2})$ here. Now its contribution to Eq. (60) is seen to be of $\mathcal{O}(1/\pi^{+3})$, whereas the predominating convective terms appear to be of $\mathcal{O}(1/\pi^{+6})$ therein. From inspection of the original wall layer equation (18), subject to the requirements (26) and (25), and matching with the flow upstream that is represented by the expansions (59), (62), and (69), the flow quantities in the core region then are easily found to be expanded in the form

$$[\Psi^+, \Sigma^+] \sim [\Psi_{00}^+, \Sigma_{00}^+](Y^+) + \pi^+[\bar{\Psi}_0^+, \bar{\Sigma}_0^+](Y^+) + \pi^+\sum\nolimits_{i=1}^{\infty}(\pi^+)^i[\hat{\Psi}_i^+, \hat{\Sigma}_i^+](\hat{s}, Y^+) + \cdots. \tag{71}$$

Herein, the sum in Eq. (71) accounts for the nonlinear convective terms in Eq. (18), where the dominant ones of $\mathcal{O}(\gamma_0/\pi^{+6})$ are those proportional to u_T within the brackets. The details of the general analysis of a mainly inviscid core region of a fluid layer with relatively small streamwise extent can be found in Ref. 2. The most important results are that the leading-order terms depend on Y^+ only and that the expressions for $\hat{\Psi}_i^+$, $i > 0$, contain eigensolutions that are proportional to $\Psi_{00}^{+\prime}$:

$$\hat{\Psi}_1^+/\Psi_{00}^{+\prime}(Y^+) = \hat{A}_1(\hat{s}) \quad (\sim a_1(-\hat{s})^{1/6} + \cdots, \quad \hat{s} \to -\infty), \tag{72}$$

$$\hat{\Psi}_2^+/\Psi_{00}^{+\prime}(Y^+) = \hat{A}_2(\hat{s}) - \hat{A}_1(\hat{s}) \int_{Y_b^+}^{Y^+} \frac{(\bar{\Psi}_0^{+\prime}\Psi_{00}^{+\prime\prime} - \bar{\Psi}_0^{+\prime\prime}\Psi_{00}^{+\prime})(\vartheta)}{[\Psi_{00}^{+\prime}(\vartheta)]^2}\,\mathrm{d}\vartheta, \tag{73}$$

$$\begin{aligned}\hat{\Psi}_3^+/\Psi_{00}^{+\prime}(Y^+) = \hat{A}_3(\hat{s}) &- \int_{Y_b^+}^{Y^+} \frac{(\bar{\Psi}_0^{+\prime}\hat{\Psi}_{2\,Y^+}^{+} - \bar{\Psi}_0^{+\prime\prime}\hat{\Psi}_2^+)(\vartheta) + [\hat{A}^2(\hat{s})/2](\Psi_{00}^{+\prime\prime 2} - \Psi_{00}^{+\prime}\Psi_{00}^{+\prime\prime\prime})(\vartheta)}{[\Psi_{00}^{+\prime}(\vartheta)]^2}\,\mathrm{d}\vartheta \\ &- 2(-\hat{s})^{1/2}\,\Psi_{00}^{+\prime}(Y^+)\left[\frac{1}{Y^+} + \int_0^{Y^+}\left(\frac{1}{\vartheta^2} - \frac{1}{[\Psi_{00}^{+\prime}(\vartheta)]^2}\right)\mathrm{d}\vartheta\right].\end{aligned} \tag{74}$$

The behavior of $\hat{A}$ in the limit $\hat{s} \to \infty$ given in Eq. (72) follows from Eq. (68). The lower bound Y_b^+ of the integrals in Eqs. (73) and (74) must be positive, in order to account for the singular behavior of the integrands due to the near-wall behavior given by (26) and (25), but otherwise can be chosen arbitrarily. The relationship (74) for $\hat{\Psi}_3^+$ is affected by the pressure gradient, cf. Eq. (62). The functions $\hat{A}_i$ are determined in the course of matching the flow quantities in the core region with that in the aforementioned sublayer, considered next.

Hence, we introduce sublayer quantities $\hat{\Psi}$, $\hat{Y}$ of $\mathcal{O}(1)$ as

$$\Psi^+ \sim \pi^{+4}\,\hat{\Psi}(\hat{s}, \hat{Y}) + \mathcal{O}(\pi^{+10}), \quad Y^+ = \pi^{+2}\,\hat{Y}. \tag{75}$$

Note that Σ^+ is seen to be of $\mathcal{O}(\pi^{+6})$ and, in turn, negligibly small in this sublayer. As a result, here the BL equations of classical, i.e. laminar, type are fully retained to leading order:

$$\hat{\Psi}_{\hat{Y}}\hat{\Psi}_{\hat{Y}\hat{s}} - \hat{\Psi}_{\hat{s}}\,\hat{\Psi}_{\hat{Y}\hat{Y}} = -(-\hat{s})^{-1/2} + \hat{\Psi}_{\hat{Y}\hat{Y}\hat{Y}}, \tag{76}$$

$$\hat{Y} = 0: \quad \hat{\Psi} = \hat{\Psi}_{\hat{Y}} = 0, \quad \hat{Y} \to \infty: \quad \hat{\Psi}_{\hat{Y}}\hat{\Psi}_{\hat{Y}\hat{s}} - \hat{\Psi}_{\hat{s}}\,\hat{\Psi}_{\hat{Y}\hat{Y}} \sim -(-\hat{s})^{-1/2}, \tag{77}$$

$$\hat{s} \to -\infty: \quad \hat{\Psi} \sim (-\hat{s})^{2/3}\zeta^2/2 + (-\hat{s})^{1/2} f(\zeta), \quad \zeta = \hat{Y}/(-\hat{s})^{1/3}\ [= \mathcal{O}(1)]. \tag{78}$$

Herein, the initial conditions for $\hat{s} \to -\infty$ provide a match with the flow in the region where $\bar{s} = \mathcal{O}(1)$ and imply $\hat{\Psi} \sim \hat{Y}^2/2 + \mathcal{O}[(-\hat{s})^{-1/6}]$ for $\hat{Y} = \mathcal{O}(1)$, in agreement with the expansion (67). The matching condition for $\hat{Y} \to \infty$, see Eq. (77), reflects the inviscid nature of the flow on top the sublayer, i.e. within the core region.

It is instructive to outline how the behavior of $\hat{\Psi}$ for $\hat{Y} \to \infty$ then can be derived solely from the conditions (78) of matching with the flow upstream. Integration of the inviscid part of Eq. (76) reveals that Bernoulli's law holds in the limit $Y^+ \to \infty$, here expressed through

$$\hat{\Psi}_{\hat{Y}}^2/2 - 2(-\hat{s})^{1/2} \sim \Phi(\hat{\Psi}), \quad \Phi'(\hat{\Psi}) = \hat{\Psi}_{\hat{Y}\hat{Y}}, \quad \hat{Y} \to \infty. \tag{79}$$

Herein, $-2(-\hat{s})^{1/2}$ and $\Phi(\hat{\Psi})$ represent, respectively, the pressure term and an at first unknown total head. By taking into account Eq. (66), one infers from matching the sublayer with the region where $\zeta = \mathcal{O}(1)$ that $\hat{\Psi} \sim \hat{Y}^2/2 - a_0\hat{Y}^{3/2} + \mathcal{O}[(-\hat{s})^{1/6}\hat{Y}]$ in the double limit $\hat{s} \to -\infty$, $\zeta \to \infty$. The first two terms of this expansion allow to determine $\Phi(\hat{\Psi})$ in the limit $\hat{\Psi} \to \infty$: since higher-order terms are inherently s-dependent and, correspondingly, lead to an additional s-dependence of Φ, they cannot contribute to the "inviscid" part of Φ. By disregarding them, integration of the second of the relationships (79) then yields $\Phi = \hat{\Psi} - 2^{-1/4}a_0\,\hat{\Psi}^{3/4}$; from subsequent integration of the first of those relationships one obtains

$$\hat{\Psi} \sim \hat{Z}^2/2 - a_0\hat{Z}^{3/2} - 2(-\hat{s})^{1/2} + \mathcal{O}\big(\hat{Z}^{-3/2}\big), \quad \hat{Z} := \hat{Y} + \hat{A}_1(\hat{s}), \quad \hat{Y} \to \infty. \tag{80}$$

In this expansion the pressure term is found as a particular solution of Eq. (79) and terms of $\mathcal{O}(\hat{Z}^{-3/2})$ are affected by the shear stress term in Eq. (76). Furthermore, the "constant" $\hat{A}_1$ of integration with respect to $\hat{Y}$ follows from a match with the core region, according to Eq. (72).

The initial-boundary value problem posed by Eqs. (76)–(78) describes a BL under the action of an adverse pressure gradient. Most important, its solution is well-known to terminate at an (a priori unknown) position $\hat{s} = \hat{s}_{\mathcal{G}} < 0$ in form of a Goldstein singularity; here we refer to Refs. 2, 9, 10, and the remarks stated by Neish and Smith[4] in connection with an akin situation that arises in their treatment of trailing-edge flow. (A thorough numerical treatment of Eqs. (76)–(78) that rigorously clarifies this property and determines the value of $\hat{s}_{\mathcal{G}}$ will be provided in a subsequent related paper.) Here we only present the most relevant results from the local analysis of these equations by considering the representative limit

$$\xi := [\omega(\hat{s}_{\mathcal{G}} - \hat{s})]^{1/4} \to 0, \tag{81}$$

where the (positive) constant ω and the value of $\hat{s}_{\mathcal{G}}$ are fixed by the solution of Eqs. (76)–(78):[9,10]

$$\hat{Y} = \mathcal{O}(1): \quad \hat{\Psi} - \hat{\Psi}_0(\hat{Y}) \sim \hat{\Psi}_0'(\hat{Y})\,\xi^2[1 + \mathcal{O}(\xi)], \quad \hat{Y} = 0: \quad \hat{\Psi}_{\hat{Y}\hat{Y}} \sim (-\hat{s}_{\mathcal{G}})^{-1/2}\,\xi^2[1 + \mathcal{O}(\xi)], \tag{82}$$

$$\hat{Y} \to 0: \quad \hat{\Psi}_0 \sim (-\hat{s}_{\mathcal{G}})^{-1/2}\,[\hat{Y}^3/6 - \omega\hat{Y}^5/240 + \mathcal{O}(\hat{Y}^6)]. \tag{83}$$

Strictly speaking, the asymptotically correct description of that singular behavior requires the introduction of a further region where $\hat{Y} = \mathcal{O}(\xi)$ or, equivalently, $\hat{\Psi} = \mathcal{O}(\xi^3)$. In turn, this Goldstein region is characterized by the distinguished limit

$$\iota := \hat{Y}/\xi = \mathcal{O}(1). \tag{84}$$

The crucial result is provided by the square–root singularity exhibited by the shear rate $\hat{\Psi}_{\hat{Y}\hat{Y}}$ evaluated at the surface in terms of $\hat{s}_G - \hat{s}$, cf. Eq. (82).

IV. Comparison with Numerical Results

IV.A. Kirchhoff-type Flow

Without going into the technical details, we note that the Kirchhoff-type potential-flow problem for the canonical case of a circular cylinder in uniform cross stream, as referred to in figure 1 on page 5 (a), has been solved numerically by employing the particular methods of conformal mapping elucidated in.[3] We now discuss the solutions displayed in figure 4. Let $\phi := 180\,x/\pi$, such that the position of $\mathcal{S}$ is characterized by the angle $\phi_{\mathcal{S}}$, which is a function of k: $\phi_{\mathcal{S}}(k)$. One then obtains $\phi_{min} := \phi_{\mathcal{S}}(0) \doteq 55^\circ\,02'\,30''$, cf. Ref. 3. In general, for a convex surface contour the BV parameter k increases for increasing values $x = x_{\mathcal{S}}(k)$, $\phi = \phi_{\mathcal{S}}(k)$. Also, the case of a body shape which is symmetric with respect to the free-stream flow direction serves as a sufficient condition that the free streamlines have the form of a parabola sufficiently far downstream of the body under consideration. Therefore, then they confine an infinitely large dead-water zone. Specifically, in the canonical case depicted here, the inflection point of the free streamlines is shifted to infinity as $k \to k_{max} \doteq 0.49079$, so that they meet asymptotically at infinity for $k = k_{max}$ and $\phi_{max} := \phi(k_{max}) \doteq 126^\circ\,43'\,32''$.

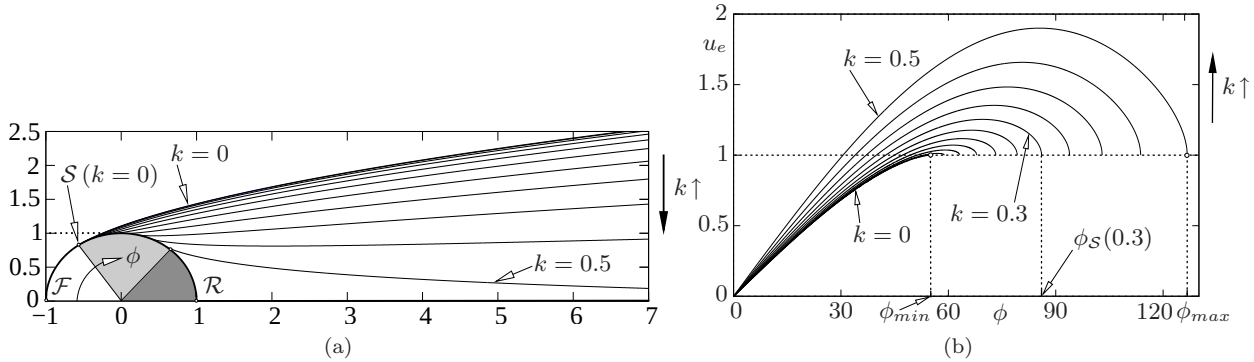

Figure 4. Kirchhoff flow around a circular cylinder for discrete values $k = i \times 0.05$, $i = 0, 1, \ldots, 10$: (a) separating streamlines (figures on axes measure horizontal and vertical distance from centre in multiples of unit radius), (b) distribution $u_e(x; k)$ over $\phi\,[^\circ]$, terminating at $x = x_D(k)$, $\phi = \phi_D(k)$ in form of the BV singularity, see Eq. (7) (e.g. $\phi_{\mathcal{S}}(0.3) \doteq 86^\circ\,1'\,54''$).

Note that $k \geq 0$ for geometrical reasons. Also, for $k \leq k_{max}$ the dead-water region is semi-infinitely open, so that there the value of the pressure equals $p_{0,\mathcal{S}}$ or, equivalently, $p_{0,\mathcal{C}}$ and that of the pressure at infinity, denoted by $p_{0,\infty}$. For $k > k_{max}$, however, the dead-water pressure $p_{0,\mathcal{S}}$ enters the problem as a further

parameter. In that case the stagnant-flow region is cusp-shaped and of finite extent, cf. Ref. 22. This type of potential flow is currently under investigation. Here we only note that the strictly attached potential flow, exhibiting a rear-stagnation point $\mathcal{R}$, considered by Neish and Smith[4] then is seen as the limit of a class of flows that show an increase of $p_{0,\mathcal{S}}$ from $p_{0,\infty}$ up to the limiting value $p_{0,\mathcal{R}}$. According to Bernoulli's law, one readily finds that $p_{0,\mathcal{S}} + u_{e,\mathcal{S}}^2/2$, with $p_{0,\mathcal{S}} = p_{0,\mathcal{C}}$ and $u_{e,\mathcal{S}} = u_{e,\mathcal{C}}$, equals the value $p_{0,\infty} + 1/2\,(= p_{0,\mathcal{F}})$ of the total head, characteristic of the free streamline $\mathcal{C}$. Furthermore, due to the strong inflection of the $\mathcal{C}$ near $\mathcal{S}$ as expressed by Eq. (10), $u_e \to 0$ in the limit $k \to \infty$. Therefore, we expect that $\mathcal{S}$ approaches $\mathcal{R}$ then. Also, in this limiting case the need of a further potential-flow region in the vicinity of $\mathcal{S}$ is indicated as the expansions (7), (9), and (10) are only valid for $|s| \ll k^{-2}$.

In the present study, however, we tacitly restrict the analysis to flows exhibiting an open cavity. This assumption agrees with the original finding of a class of potential flows that are only parametrized by k, as already mentioned in § II. Both the regimes of the values of k that refer to an open and closed stagnant-flow region, respectively, are indicated by the light- and dark-shaded sectors in figure 4 (a).

IV.B. Boundary Layer Flow

IV.B.1. Asymptotically Correct Reynolds Stress Closure

In order to obtain numerical solutions of the BL problem posed by Eqs. (12)–(15) for various values of k and T, the Reynolds shear stress function Σ is conveniently modelled on the basis of the mixing length formulation, which is associated with the concept of a rather sharp BL edge $Y = \delta$, cf. Ref. 13. In addition, in the case $T \to \infty$ the solutions shall assume a behavior that is compatible with the asymptotic structure of the BL derived in § III. This is achieved if the mixing length is modelled as proportional to the "turbulent" BL thickness δ times a shape function, here denoted by ℓ, which is taken as the product of the two "lengths", l and l^+. These account for the BL flow in the outer main region and the viscous sublayer, respectively,

$$\Sigma = [\delta\,\ell\,\Psi_{YY}(x, Y; k, T)]^2, \quad \ell = l(\eta)\,l^+(Y^+), \tag{85}$$

$$l := \mu\,I(\zeta)^{1/2}\tanh[\kappa\,\eta/c_\ell], \quad I := 1/(1 + 5.5\,\eta^6), \quad \mu := 0.085, \tag{86}$$

$$l^+ := 1 - \exp(-Y^+/\Gamma), \quad \Gamma := \beta\,[1 - \exp(-Y^+/\varphi)]^{1/2}, \quad \beta := 27.8, \quad \varphi := 4.8\,. \tag{87}$$

In these relationships η is defined according to Eq. (30), where δ is appropriately determined as the minimum value of Y where Σ is found to be numerically insignificantly small. The expression for l in Eq. (86) is a modification of the well-known model by Michel, Quémard, and R. Durant[23] (see also Ref. 13, p. 557), where the usual intermittency factor I by Klebanoff[24] has been included. In turn, the associated pronounced decrease of ℓ eliminates the deficiency of the original model to overestimate the turbulence intensities near the BL edge. The sublayer closure[25] provided by Eq. (87) predicts the correct near-wall behavior given by Eqs. (13), (25), and (26). In Eqs. (85)–(87) the turbulent reference velocity u_T enters the definition of the wall layer coordinate Y^+, given by Eq. (16), in the form $u_T := \kappa\tau u_e$, according to Eqs. (22) and Eq. (38), rather than by adopting the original definition Eq. (17). This advantageously agrees with the asymptotic structure near separation discussed in § III.B without encountering an unbounded increase of the wall layer thickness as $u_T \to 0$ for $s \to 0_-$.

Formally, Eqs. (85)–(87) represent an appropriate mixing length closure for in the fully turbulent case, expressed by the limit $T \to \infty$. In this limit it enforces the transition towards the small-defect BL, considered in § III.A, as Eqs. (86) and (87) provide a common overlap of the main and the sublayer as it predicts the widely believed linear variation of ℓ with distance from the wall in the overlap domain, $\ell \sim \kappa\eta$, which is usually argued for by bringing forward dimensional reasoning.[13] This fully agrees with the form of the closure already addressed in § III.B.1 and expressed through Eqs. (39) and (51). In turn, the overlap behavior given by Eqs. (27), (28), and (34), is revealed. Specifically, applying the above model to the "universal" sublayer functions $\Psi_{00}^+(Y^+)$ and $\Sigma_0^+(Y^+)$ yields $vSi_0^+ = [\kappa\,Y^+ l^+ \Psi_{00}^{+\prime\prime}(Y^+)]^2$, so that Ψ_0^+ then follows from (numerical) integration of the first of the Eqs. (24), subject to the no-slip condition, see Eq. (13). Setting $\kappa = 0.384$[18] here gives $B^+ \doteq 4.8831$ and $\Sigma_0^+ \sim \varepsilon_{00} Y^{+3} + O(Y^{+\,7/2})$ with $\varepsilon_{00} \doteq 9.16 \times 10^{-4}$. That is, the near-wall behavior given by Eqs. (25) and (26) is satisfied, in numerically good agreement with experimental findings.[25,26]

IV.B.2. Partially Developed Turbulent Boundary Layer near Separation

For a numerical treatment of Eqs. (12)–(15), these equations have been suitable transformed in order to capture the smooth transition towards the Hiemenz flow as $x \to 0_+$. This procedure is presented in Ref. 1. Solutions of the transformed equations have been achieved by adopting the method of lines and employing a Keller–Box-type discretisation, supplemented with automated adaptive step control in the x-direction and an automated remeshing strategy regarding the grid in Y-direction. The latter was resolved by using approximately 10^4 grid points.

Solutions have been found by prescribing Kirchhoff-type potential flows with an open cavity, i.e. for $0 \leq k \geq k_{max}$ and for a wide range of values of T. The solutions corroborate the conjecture that the position $x = x_{\mathcal{G}}$ of the Goldstein singularity triggered by the BV singularity, see Eq. (7), is shifted downstream for increasing values of k, thereby increasing in strength. Increasing values of T, i.e. increasing turbulence intensities, are expected to foster that downstream shift as turbulent BLs are empirically known to be less prone to separate than laminar ones for identical external-flow configurations (i.e. for identical values of k). In the following, we solely discuss the solutions obtained for the specific value $k = 0.3$, which exhibit the rather surprising property that the strength of the Goldstein-singularity weakens for increasing values of T: from this scenario one then infers (needless to say, with some caution) that for a certain range of values of k (within the interval $0 < k < k_{max}$ in case of the circular cylinder) the Goldstein singularity vanishes for critical values of T.

The condition of matching with the external flow has been satisfied numerically at $Y = \delta$ within the range $10 \leq \delta \leq 100$, where δ has been increased properly for increasing values of the parameter T. The latter is varied from $T = 0$ up to $T = 10^5$; higher values result in numerical difficulties which could only be overcome by employing a considerably higher grid resolution. Hence, the BV singularity is seen to take place at $\phi = \phi_{\mathcal{S}} \doteq 86^\circ\, 1'\, 54''$, as indicated in figure 4 on page 18 (b) and figure 5 by vertical dotted lines. The resulting distributions for the reduced wall shear stress, Ω, together with that for the displacement thickness, Υ, defined by

$$\Omega(x;k,T) := \Psi_{YY}(x, Y=0;k,T)/u_e(x;k), \quad \Upsilon(x;k,T) := \int_0^\infty (1 - \Psi_Y/u_e)\,\mathrm{d}Y, \tag{88}$$

are plotted in the last figure.

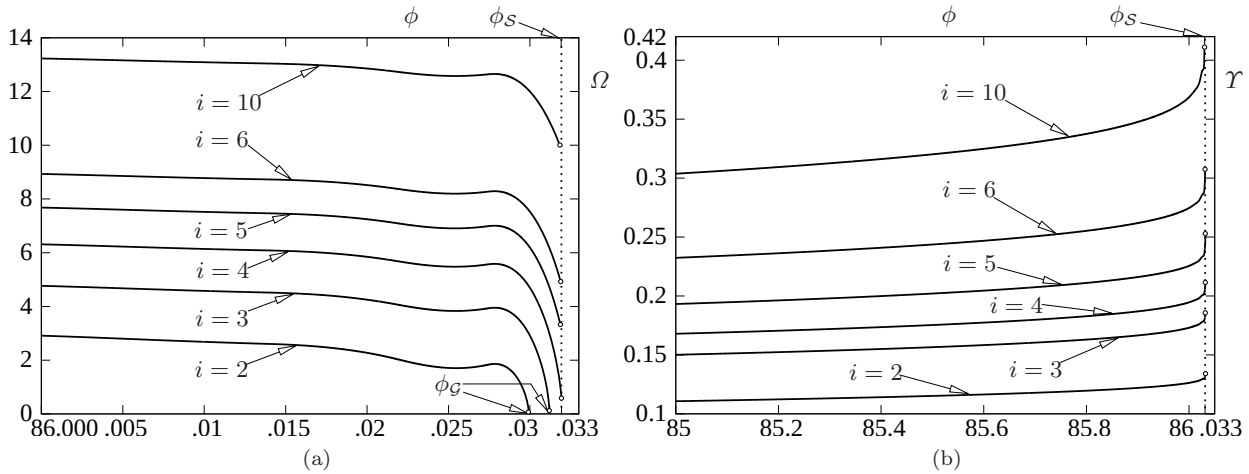

Figure 5. Key quantities of solutions of BL equations (12)–(15), for $k = 0.3$ and $T = i \times 10^4$ over arc angle $\phi\,[^\circ]$ as $\phi - \phi_{\mathcal{S}}(k) \to 0_-$, terminating at $\phi = \phi_{\mathcal{G}}(k,T)$ (positions indicated by circles): (a) reduced wall shear stress Ω, (b) displacement thickness Υ.

For sufficiently small value of T the BL behaves still laminar-like as the corresponding solutions are found to terminate in form of a Goldstein-type singularity at the location $\phi = \phi_{\mathcal{G}}(k,T)$, i.e. for $x = x_{\mathcal{G}}(k,T)$. That is, $\Omega(x;k,T) - (x_{\mathcal{G}};k,T)$ and $\Upsilon(x;k,T) - \Upsilon(x_{\mathcal{G}};k,T)$, respectively, vary with $(\phi_{\mathcal{G}} - \phi)^{1/2}$ to leading order as $\phi - \phi_{\mathcal{G}} \to 0_-$, in agreement with the analytical results of § III.B.3. Furthermore, $\phi = \phi_{\mathcal{G}}$ approaches $\phi = \phi_{\mathcal{S}}$ for increasing values of T. Eventually, when T assumes a certain value, say $T = T_{\mathcal{S}}(k)$ (here $T_{\mathcal{S}} \times 10^{-4}$ is slightly below 4), $\phi_{\mathcal{G}}(T_{\mathcal{S}}, k) = \phi_{\mathcal{S}}(k)$. In turn, for $T \geq T_{\mathcal{S}}$ the boundary-layer calculations break down at $\phi = \phi_{\mathcal{S}}(k)$, where Ω exhibits a finite limit. In fact, for $k = 0.3$ the numerical results obtained for relatively

large values of T strongly suggest a regular local behaviour of the solutions. Consequently, the fully turbulent BL obtained in the limit $T \to \infty$ having a velocity defect of $O(1/\ln T)$, would not separate at all. This result is entirely in line with the analytical investigation given in Ref. 6, which applies to the outer defect layer of a generic turbulent BL with an asymptotically small velocity deficit as $\phi - \phi_{\mathcal{S}} \to 0_-$, i.e. for $x - x_{\mathcal{S}} \to 0_-$. However, it apparently contradicts the analytically obtained results of § III.B.

V. Conclusions and Further Outlook

The present analysis is initiated by the assumption that, in the limit Eq. (1), the BL that stretches from $\mathcal{F}$ towards the point $\mathcal{S}$ of detachment of the free streamline is highly turbulent. Within the framework of BL theory this flow is governed by the Eqs. (12)–(15) for large values of T and under the action of a pressure gradient $-u_e u_{ex}$ that is impressed by the external Kirchhoff-type flow, parametrized by the BV parameter k. It has been shown in Ref. 1 that, in the limit $T \to \infty$, such a BL assumes the well-accepted two-tiered splitting. Furthermore, the existence of a front-stagnation point of the external potential flow ensures that $T \ll Re^{1/2}$. The hypothetical limit $T = Re^{1/2}$ pertains to a fully developed turbulent BL, where the viscous wall layer is characterized by a perfect equilibrium between the total and the wall shear stress to leading order. Moreover, we have demonstrated here that in this limit the strength of the Goldstein singularity that is induced by the rather abrupt pressure rise, expressed by Eq. (7), increases whereas the distance between its position and that of the BV singularity decreases asymptotically. This behavior is conveniently expressed by recasting the behavior of $\hat{\Psi}_{\hat{Y}\hat{Y}}$ for $\hat{Y} = 0$ given in Eq. (82) with the aid of Eqs. (16), (57), (58), (70), (75), and (81),

$$\Psi_{YY}(x, Y = 0; k, T) \sim T\gamma_0^6 (u_{e,\mathcal{S}}^{3/2}/k^3)[(\omega/\hat{s}_{\mathcal{G}})(x - x_{\mathcal{G}})]^{1/2} \quad (x \to x_{\mathcal{G}\_}), \quad x_{\mathcal{S}} - x_{\mathcal{G}} = \mathcal{O}[k^6/(T^8\gamma_0^{16}u_{e\mathcal{S}}^4)]. \quad (89)$$

It is also seen from these relationships that for sufficiently large but fixed values of T the strength of the Goldstein singularity decreases further, accompanied by a corresponding shift of $\mathcal{G}$ towards $\mathcal{S}$, in the limit $k \to 0_+$ that refers to laminar massive separation.[2,7,8] Contrarily, in the limit $k \to \infty$, i.e. for $u_{e,\mathcal{S}} \to 0$ as $\mathcal{S}$ is shifted towards $\mathcal{R}$, which is associated with the problem of trailing-edge flow considered in Refs. 4 and Ref. 6, the singularity decreases in strength whereas the breakdown of the BL equations is correspondingly delayed. Most important, as a consequence of the streamwise velocity defect of $\mathcal{O}(1/\ln T)$ that characterizes the outer main portion of the BL, this region is found to be largely unaffected by the singular behavior expressed in Eq. (89): it exhibits a perturbation about the terminal velocity profile, expressed by $F_{0\eta}(\eta; k)$, which is essentially of $\mathcal{O}[(-s)^{1/2}]$, see Eq. (40).

It is quite interesting that this theoretically predicted behavior of a turbulent BL slightly upstream of separation is strongly supported by the interpretation of experimental findings as well as numerical solutions of the BL equations based on commonly employed turbulence closure schemes, see Tsahalis and Telionis.[27] One should concede, however, albeit with some reservation, that the numerical results presented in § IV.B do not exclude the possibility that the Goldstein singularity is avoided for certain values of k. To the authors' present opinion, this situation is closely related to the suppression of eigensolutions that trigger the asymptotic splitting of the wall layer flow elucidated in § III.B.2. Of course, further research is required to shed light on the possibility of a second, different type of separation associated with this behavior.

Needless to say, however, an asymptotically correct description of the separation process requires an investigation of the full Reynolds-averaged equations of motion (2)–(4). Such a theory is presumably devised by exploiting the triple-deck formalism,[2] in order to take into account locally strong viscous/inviscid interaction in the vicinity of $\mathcal{S}$. The consequences of such a strategy include, amongst others, a distinguished limit $T = T(Re)$ as $T \to \infty$ and $Re \to \infty$ and were already alluded to by Neish and Smith,[4] who propose $T = \mathcal{O}(Re^{-1/18})$ for the case $0 < k < \infty$ of interest here. They arrive at this conclusion by exploiting scaling arguments and the assumption that the canonical triple-deck problem describing laminar break-away separation, established by Sychev[7] and originally solved numerically by Smith[8] (see also Ref. 2), can even be applied to the developed turbulent case. The latter property apparently has a profound basis as the region of nonlinear breakdown discussed in § III.B.3 then plays the role of the lower deck. In our point of view, however, their conclusion seems tentative for three reasons: first, their finding does not properly take into account the logarithmic law of the wall (28) and the inherently associated asymptotically small velocity deficit in the upper deck that is located at the base of the outer main region of the BL. Secondly, as has been demonstrated by Melnik and Chow,[28] the BL approximation ceases to be valid already in a region of streamwise extent of $\mathcal{O}(T\gamma)$ that compares with the BL thickness, according to Eq. (16), and where the

effect of the pressure gradient acting normal to the surface becomes important. Third, it is not clear for the time being how turbulence alters the downstream conditions that supplement the original triple-deck problem and account for the development of a separated shear layer and the region of weak reverse flow. These issues are topics of the ongoing research. Here we only give a rather coarse estimate for an upper bound of T: since the governing equations (2), (3) are required to reduce to a BL approximation in the lower deck, its streamwise extent must be asymptotically larger than that perpendicular to the surface in the limit (1). One deduces from Eqs. (11), (30), (38), (57), (58), and (70) that the former is of $\mathcal{O}[Re^{-1/2}(T\gamma_0)^{-1}]$ and the latter of $\mathcal{O}(T^{-4}\gamma_0^{-14})$, giving $T \ll Re^{1/6}(\ln Re)^{13/3}$. The most interesting feature, however, of the interaction problem to be derived concerns uniqueness of its solution. As in the laminar case,[8,29,30] it is very likely that a solution only exists for a single value of $0 < k < \infty$ which remains the only parameter entering that problem. Hence, in contrast to the laminar case where the solution approximately fixes the value of $kRe^{1/16}$ as $Re \to \infty$, for a developed turbulent BL the position of $\mathcal{S}$ on the body surface and hence the global potential flow is presumably selected by the solution of the local interaction problem.

A BL description akin to that presented here likely applies also to a further related topic of interest from the point of view of aerodynamics, namely, turbulent trailing edge-flow past a plate under angle of attack, then measured by k. Here we refer the preliminary asymptotic results given by Melnik and Chow.[28] Most important, it is very likely that a rational description of separation then also predicts a maximum level of turbulence intensity in the oncoming attached BL. As a remarkable – although tentative – conclusion drawn from these considerations is that the Reynolds stresses in a turbulent BL along a body of finite dimensions that undergoes break-away separation never exhibit their theoretically maximum possible magnitude, associated with the well-established two-tiered fully developed turbulent BL that was described in a self-consistent manner by Mellor[5] and is recovered in the case $T = Re^{1/2}$. A discussion of the consequences of this finding are certainly beyond the scope of the present analysis. However, it is corroborated by the fact that for fully developed turbulent flow the viscous wall layer is exponentially thin compared to the outer defect layer as these regions have thicknesses of $\mathcal{O}(\ln Re/Re)$ and $\mathcal{O}(1/\ln Re)$, respectively, cf. Eqs. (16), (30), by noting that $\sigma = \gamma$, and (38): that is, the triple-deck structure then does not apply here as the displacement exerted by the lower deck located in the wall layer is too weak to generate a sufficiently large pressure feedback in the same region which originates from the upper deck in the small defect-region. It seems that such a BL withstands a pressure rise that is associated with a value of k of $\mathcal{O}(1)$, cf. Eq. (7), which, however, contradicts the basic assumption of free streamline originating in $\mathcal{S}$. In turn, it is felt that a proper coupling between k, T, and Re in the aforementioned case $k \to \infty$ implies larger values of T than those allowed in the case $k = \mathcal{O}(1)$, which is also indicated by Eq. (89). A treatment of this type of trailing-edge flow, based on the preceding analysis given in Refs. 4, 6, will be presented in a subsequent study.

Acknowledgments

Special thanks are due to Professor Frank T. Smith (Department of Mathematics, University College London, London, UK) for frank and stimulating discussions.

References

[1]Scheichl, B., Kluwick, A., and Alletto, M., ""How Turbulent" is the Boundary Layer Separating from a Bluff Body for Arbitrarily Large Reynolds Numbers?" *Acta Mechanica*, 2008, Special issue on the occasion of the 70th birthday of Professor Wilhelm Schneider, accepted for publication.

[2]Sychev, V. V., Ruban, A. I., Sychev, Vic. V., and Korolev, G. L., *Asymptotic Theory of Separated Flows*, edited by A. F. Messiter and M. Van Dyke, Cambridge University Press, Cambridge, UK, 1998.

[3]Gurevich, M. I., *The Theory of Jets in an Ideal Fluid*, Vol. 93 of Int. Series of Monographs in Pure and Applied Mathematics, Pergamon Press, Oxford, 1966, original Russian book: 1961, Moscow: Fizmatlit.

[4]Neish, A. and Smith, F. T., "On Turbulent Separation in the Flow past a Bluff Body," *Journal of Fluid Mechanics*, Vol. 241, Aug. 1992, pp. 443–467.

[5]Mellor, G. L., "The Large Reynolds Number, Asymptotic Theory of Turbulent Boundary Layers," *International Journal of Engineering Science*, Vol. 10, No. 10, 1972, pp. 851–873.

[6]Scheichl, B. and Kluwick, A., "Asymptotic Theory of Bluff-Body Separation: A Novel Shear-Layer Scaling Deduced from an Investigation of the Unsteady Motion," *Journal of Fluids and Structures*, Vol. 24, No. 8, Dec. 2008, Special issue on the IUTAM Symposium on Separated Flows and their Control, accepted for publication.

[7]Sychev, V. V., "Laminar Separation," *Fluid Dynamics*, Vol. 7, No. 3, 1972, pp. 407–417, original Russian article in *Izv. Akad. Nauk SSSR, Mekh. Zhidk. i Gaza* (3), 1972, 47–59.

[8]Smith, F. T., "The Laminar Separation of an Incompressible Fluid Streaming past a Smooth Surface," *Proceedings of the Royal Society of London* A, Vol. 356, No. 1687, 1977, pp. 443–463.

[9]Goldstein, S., "On Laminar Boundary Layer Flow near a Position of Separation," *The Quarterly Journal of Mechanics and Applied Mathematics*, Vol. 1, No. 1, 1948, pp. 43–69.

[10]Stewartson, K., "Is the singularity at separation removable?" *Journal of Fluid Mechanics*, Vol. 44, No. 2, Nov. 1970, pp. 347–364.

[11]Schewe, G., "Reynolds-number Effects in Flows Around More-or-less Bluff Bodies," *Journal of Wind Engineering & Industrial Aerodynamics*, Vol. 89, No. 14, 2001, pp. 1267–1289.

[12]Zdravkovich, M. M., *Flow Around Circular Cylinders. A Comprehensive Guide Through Flow Phenomena, Experiments, Applications, Mathematical Models, and Computer Simulations. Vol. 1: Fundamentals*, Oxford University Press, Oxford, New York, Tokyo, 1997.

[13]Schlichting, H. and Gersten, K., *Boundary-Layer Theory*, Springer-Verlag, Berlin, Heidelberg, Germany, 8th ed., 2000.

[14]Walker, J. D. A., Abbott, D. E., Scharnhorst, R. K., and Weigand, G. G., "Wall-Layer Model for the Velocity Profile in Turbulent Flows," *AIAA Journal*, Vol. 27, No. 2, Feb. 1989, pp. 140–149.

[15]Walker, J. D. A., "Turbulent Boundary Layers II: Further Developments," *Recent Advances in Boundary Layer Theory*, edited by A. Kluwick, Vol. 390 of *CISM Courses and Lectures*, Springer-Verlag, Vienna, New York, 1998, pp. 145–230.

[16]Scheichl, B. and Kluwick, A., "Turbulent shear-layer scaling in the limit of infinite Reynolds number derived from the unsteady equations of motion," *Proceedings of Applied Mathematics and Mechanics (PAMM)*, Vol. 7, No. 1, Dec. 2007, Special Issue: GAMM Annual Meeting 2007 – Zürich, accepted for publication.

[17]Scheichl, B. and Kluwick, A., "On turbulent marginal boundary layer separation: how the half-power law supersedes the logarithmic law of the wall," *International Journal of Computing Science and Mathematics (IJCSM)*, Vol. 1, No. 2/3/4, 2007, pp. 343–359, Special Issue on Problems Exhibiting Boundary and Interior Layers.

[18]Österlund, J. M., Johansson, A. V., Nagib, H. M., and Hites, M., "A Note on the Overlap Region in Turbulent Boundary Layers," *Physics of Fluids*, Vol. 12, No. 1, 2000, pp. 1–4, Letter.

[19]Scheichl, B. and Kluwick, A., "Turbulent Marginal Separation and the Turbulent Goldstein Problem," *AIAA Journal*, Vol. 45, No. 1, Jan. 2007, pp. 20–36, see also *AIAA paper 2005-4936*.

[20]Abramowitz, M. and Stegun, I. A., *Handbook of Mathematical Functions*, Dover Publications, New York, 9th ed., 1972.

[21]Messiter, A. F. and Enlow, R. L., "A Model for Laminar Boundary-Layer Flow near a Separation Point," *SIAM Journal on Applied Mathematics*, Vol. 25, No. 4, Dec. 1973, pp. 655–670.

[22]Southwell, R. V., F.R.S. and Vaisey, G., "Relaxation Methods Applied to Engineering Problems. XII. Fluid Motions Characterised by 'Free' Streamlines," *Phil. Trans. R. Soc. Lond.* A, Vol. 240, No. 815, Nov. 1946, pp. 117–161.

[23]Michel, R., Quémard, C., and Durant, R., "Hypothesis on the Mixing Length and Application to the Calculation of the Turbulent Boundary Layers," *Proceedings of Computations of Turbulent Boundary Layers – 1968 AFOSR-IFP-Stanford Conference. Methods, Predictions, Evaluation and Flow Structure*, edited by S. J. Kline, M. V. Morkovin, G. Sovran, and D. J. Cockrell, Vol. 1, Stanford University, Stanford, CA, 1969, pp. 195–207.

[24]Klebanoff, P. S., "Characteristics of Turbulence in a Boundary Layer with Zero Pressure Gradient," NACA Rept. 1247, NASA – Langley Research Center, Hampton, VA, 1955, see also NACA TN 3178, 1954.

[25]Grifoll, J. and Giralt, F., "The Near Wall Mixing Length Revisited," *International Journal of Heat and Mass Transfer*, Vol. 43, No. 19, 2000, pp. 3743–3746, Technical Note.

[26]Kays, W. M., "Turbulent Prandtl Number – Where Are We?" *ASME Journal of Heat Transfer*, Vol. 116, No. 2, May 1994, pp. 284–295.

[27]Tsahalis, D. T. and Telionis, D. P., "On the Behavior of Turbulent Boundary Layers near Separation," *AIAA Journal*, Vol. 13, No. 10, Oct. 1975, pp. 1261–1262, Synoptics.

[28]Melnik, R. E. and Chow, R., "Asymptotic Theory of Two-Dimensional Trailing-Edge Flow," Nas-1-12426, Grumman Aerospace Corporation, NASA – Langley Research Center, Hampton, VA, 1975.

[29]Korolev, G. L., "Numerical Solution of the Asymptotic Problem of Laminar Boundary-Layer Separation from a Smooth Surface," *Uch. zap. TsAGI*, Vol. 11, No. 2, Feb. 1980, pp. 27–36.

[30]van Dommelen, L. L. and Shen, S. F., "Interactive Separation from a Fixed Wall," *Numerical and Physical Aspects of Aerodynamic Flows II, Proceedings of the 2nd Symposium held at California State University, Long Beach, CA, 17–20 January, 1983*, edited by T. Cebeci, Springer-Verlag, New York, Berlin, Heidelberg, Tokyo, 1984, pp. 393–402.